Elsevier Editorial System(tm) for Marine and Petroleum Geology

Manuscript Draft

Manuscript Number: JMPG-D-19-00328R1

Title: Sedimentary evolution of a shallow carbonate ramp (Kimmeridgian, NE Spain): unravelling controlling factors for facies heterogeneities at reservoir scale

Article Type: Full Length Article

Keywords: Shallow carbonate ramp; Kimmeridgian; Iberian Basin; facies heterogeneities; hydrocarbon reservoir analogue

Corresponding Author: Mrs. Cristina Sequero, Ph.D. Student

Corresponding Author's Institution: University of Zaragoza

First Author: Cristina Sequero, Ph.D. Student

Order of Authors: Cristina Sequero, Ph.D. Student; Marcos Aurell, Full Professor; Beatriz Bádenas, Professor

Abstract: The facies evolution of a Late Jurassic (latest Kimmeridgian) shallow carbonate ramp was reconstructed after the analysis and correlation of 21 logs in a 20 x 30 km outcrop area located south of Zaragoza (northeast Spain). The studied succession belongs to the Higueruelas Formation, which is of potential use as an analogue for understanding facies heterogeneities in certain hydrocarbon carbonate reservoirs (e.g. the Arab Formation, Persian Gulf). The studied succession is arranged in nine sedimentary units bounded by discontinuity surfaces that can be traced over kilometres. Facies analysis permitted the reconstruction of two sedimentary models showing the transition from inner ramp subenvironments (i.e. intertidal, lagoon, backshoal/washover, shoal-sand blanket) to the mid-ramp foreshoal and offshore domains: an oncolitic-peloidal-oolitic and an oolitic-peloidal-dominated ramp. The oncolitic-peloidal-oolitic-dominated ramp is characterized by peloidal-oolitic and oncolitic-dominated shoal-sand blankets that developed in higher-energy inner areas, protecting peloidal-oolitic backshoal and oncolitic lagoon domains including a mosaic of stromatoporoid carpets. Peloidal facies with fenestral porosity accumulated in an intertidal belt or as patches on top of the shoal-sand blankets and washover deposits. Offshore from the shoal-sand blankets, chaetetid/stromatoporoid/coral-rich buildups grew on the more proximal mid-ramp, surrounded by peloidal and peloidal-bioclastic grain- to mud-supported facies. An oolitic-peloidal-dominated ramp developed in a second stage of the evolution of the platform, characterized by the presence of a wide restricted peloidal-bioclastic-oolitic lagoon on the inner ramp grading into a backshoal area dominated by storm-related intraclastic-peloidal deposits. Stromatoporoid carpets disappeared and oncolitic-dominated deposits were constrained to the foreshoal and backshoal domains, and locally to local ponds that developed in the intertidal belt or the restricted lagoon. Internal and external factors controlling facies heterogeneity and the sedimentary evolution of the carbonate ramp include resedimentation, topographic relief, and long- to short-term sea-level fluctuations.

Research Data Related to this Submission

There are no linked research data sets for this submission. The following reason is given:
No data was used for the research described in the article

Sedimentary evolution of a shallow carbonate ramp (Kimmeridgian, NE Spain): unravelling controlling factors for facies heterogeneities at reservoir scale

Cristina Sequero*, Marcos Aurell, Beatriz Bádenas

Departamento de Ciencias de la Tierra-IUCA, Universidad de Zaragoza, 50009-Zaragoza, Spain

*Corresponding author: cristinasq92@gmail.com

Abstract

The facies evolution of a Late Jurassic (latest Kimmeridgian) shallow carbonate ramp was reconstructed after the analysis and correlation of 21 logs in a 20 x 30 km outcrop area located south of Zaragoza (northeast Spain). The studied succession belongs to the Higueruelas Formation, which is of potential use as an analogue for understanding facies heterogeneities in certain hydrocarbon carbonate reservoirs (e.g. the Arab Formation, Persian Gulf). The studied succession is arranged in nine sedimentary units bounded by discontinuity surfaces that can be traced over kilometres. Facies analysis permitted the reconstruction of two sedimentary models showing the transition from inner ramp subenvironments (i.e. intertidal, lagoon, backshoal/washover, shoal-sand blanket) to the mid-ramp foreshoal and offshore domains: an oncolitic-peloidal-oolitic and an oolitic-peloidal-dominated ramp. The oncolitic-peloidal-oolitic-dominated ramp is characterized by peloidal-oolitic and oncolitic-dominated shoal-sand blankets that developed in higher-energy inner areas, protecting peloidal-oolitic backshoal and oncolitic lagoon domains including a mosaic of stromatoporoid carpets. Peloidal facies with fenestral porosity accumulated in an intertidal belt or as patches on top of the shoal-sand blankets and washover deposits. Offshore from the shoal-sand blankets, chaetetid/stromatoporoid/coral-rich buildups grew on the more proximal mid-ramp, surrounded by peloidal and peloidal-bioclastic grain- to mud-supported facies. An oolitic-peloidal-dominated ramp developed in a second stage of the evolution of the platform, characterized by the presence of a wide restricted peloidal-bioclastic-oolitic lagoon on the inner ramp grading into a backshoal area dominated by storm-related intraclastic-peloidal deposits. Stromatoporoid carpets disappeared and oncolitic-dominated deposits were constrained to the foreshoal and backshoal domains, and locally to local ponds that developed in the intertidal belt or the restricted lagoon. Internal and external factors controlling facies heterogeneity and the sedimentary evolution of the carbonate ramp include resedimentation, topographic relief, and long- to short-term sea-level fluctuations.

Keywords

Shallow carbonate ramp, Kimmeridgian, Iberian Basin, facies heterogeneities, hydrocarbon reservoir analogue

1. Introduction

Reconstruction of facies heterogeneities on epeiric shallow carbonate ramps is difficult due to the absence of recent analogues as well as to the complexity of the interacting factors that controlled the facies distribution and sedimentary evolution (e.g. Burchette and Wright, 1992; Bádenas and Aurell, 2010; Pomar, 2018). A particular point of interest in studying ancient epeiric shallow carbonate ramps is the definition of the lateral and vertical extent of carbonate bodies. A significant difference between epeiric ramps and rimmed platforms is the wide lateral extension of the facies belts, and in particular of carbonate sand bodies, in the former (Burchette and Wright, 1992). Rimmed platforms are limited in their progradation by the bordering deep ocean, whereas in ramps the potential for progradation of the carbonate sand shoals over the low-angle depositional slope results in much greater extension and potential for preservation of grain-supported facies (Droste, 2006; Bádenas and Aurell, 2010). A knowledge of the geometry and lateral continuity of porous and permeable grain-supported facies and their relationship with mud-supported facies is a key aspect of reservoir exploration and development strategies in ancient carbonate platforms (e.g. Borkhataria et al., 2005).

Outcrop analogue studies play an essential role in unravelling the internal heterogeneities of subsurface shallow carbonate systems, and the construction of depositional models is a condition for evaluating carbonate reservoirs (Pomar et al., 2015). In carbonate rocks, the study of outcrop analogues is of additional interest due to the dependence of sediment production upon carbonate-producing organisms and, consequently, the reliance of carbonate production on environmental conditions. Numerous modern analogue studies of shallow marine environments (Wilkinson et al., 1999; Rankey and Reeder, 2011; Harris et al., 2014; Purkis et al., 2015) have revealed important heterogeneities in facies distribution controlled by a range of factors such as sea-level fluctuations and hydrodynamic conditions, as well as by changes in carbonate-producing biota, which are controlled in turn by their ecological requirements, such as temperature, ocean chemistry and nutrient availability (Pomar and Kendall, 2007; Strasser and Védrine, 2009; Harris et al., 2014; Hönig and John, 2015). In the case of carbonate ramps, several works have demonstrated that despite their usually well-defined facies belts, these facies belts can vary laterally (along strike and along dip), and facies mosaics in some ramp subenvironments can also develop in relation with biological and hydrodynamic factors (e.g. Bádenas et al., 2010; Tomás et al., 2010; Amour et al., 2013; San Miguel et al., 2017a; Tomassetti et al., 2018), thus complicating the heterogeneity and predictability of the facies. More studies on carbonate ramp systems are thus required to unravel the distribution of rock bodies for further 3D modelling of volume and/or fluid-flow assessment.

The shallow facies of the late Kimmeridgian carbonate ramp that developed in the north-central part of the Iberian Basin are of particular interest due to the wide record of skeletal and non-skeletal grains similar to those found in the most important hydrocarbon carbonate reservoirs worldwide (i.e. the Arab-D Fm, Persian Gulf; Al-Awwad and Collins, 2013). The main purpose of the present work is to characterize the facies distribution and sedimentary evolution of this shallow carbonate ramp exposed in the outcrops south of Zaragoza (Iberian Basin, NE Spain). Bed-by-bed facies analysis and the correlation of closely-spaced logs provide a precise scheme showing the vertical and lateral (along strike and along dip) facies distribution. This allows the dimensions of the facies belts to be ascertained, as well as the lateral distribution (from inner- to mid-ramp) of the more common non-skeletal components (peloids, ooids, oncoids, intraclasts) and the preferential growth of stromatoporoid carpets and chaetetid-stromatoporoid-

coral buildups. On the basis of the relative proportions of the more common non-skeletal grains, two sedimentary models are proposed. These models are of potential interest for improving subsurface interpretations of carbonate ramps, in particular with respect to dimensions and internal heterogeneities of reservoir-rock bodies.

2. Geological setting and stratigraphy

During the Kimmeridgian (Late Jurassic), shallow epeiric seas covered wide areas of western Europe (Fig. 1A). Terrigenous sedimentation occurred to the north and west, whereas carbonate sedimentation was dominant on eastern and northeastern platforms facing the Tethys Ocean (Decourt et al., 1993). A large part of the Iberian Plate was uplifted, forming the Iberian Massif. To the east of this massif, wide carbonate ramps developed during the Kimmeridgian in the so-called Iberian Basin, an intra-cratonic basin that originated during the Mesozoic extensional phase (Fig. 1B; Salas and Casas, 1993; Aurell et al., 2003, 2010). These carbonate ramps were affected by NW-directed hurricanes and winter winds (Bádenas and Aurell, 2001), in accordance with the palaeoclimate models proposed by Marsaglia and Klein (1983) and Price et al. (1995) (Fig. 1B).

During the Kimmeridgian, the Iberian Basin displays a sedimentary evolution characterized by low-angle carbonate ramps recorded increasingly towards the eastern areas of the basin, due to a long-term fall in relative sea level that was partly controlled by the tectonic uplift of the Iberian Massif (Bádenas and Aurell, 2001; Aurell et al., 2003). These carbonate ramp successions are arranged in three third-order depositional sequences (sequences Ki1, Ki2 and Ki3; Fig. 1C; Aurell et al., 2010, in press). Sequences Ki1 and Ki2 correspond to shallow oolitic and reefal facies (Ricla Mb and Torrecilla Fm), passing down dip into the mid- and outer-ramp marls and lime mudstones of the Sot the Chera and Loriguilla formations (Bádenas and Aurell, 2001; Aurell et al., 2010). The stratigraphic succession studied here belongs to the latest Kimmeridgian sequence Ki3, represented in the north-central part of the Iberian Basin by the shallow-water carbonate deposits of the Higueruelas Fm (Aurell and Meléndez, 1986, 1987; Ipas et al., 2004; Aurell et al., 2010). This unit has a wide range of grain-supported facies characterized by a predominance of non-skeletal grains (mainly oncoids, but also ooids, peloids, intraclasts and aggregate grains) and also includes small carpets and buildups of corals, chaetetids and stromatoporoids (e.g. Bádenas and Aurell, 2003; Aurell et al., 2012; Sequero et al., 2018). The latest Kimmeridgian age attributed to the Higueruelas Fm is based on the widespread record of the benthic foraminifera *Alveosepta jaccardi* combined with the presence of mid-Kimmeridgian ammonites (i.e. *acanthicum*/*eudoxus* zones) in the underlying Loriguilla Fm (Bádenas et al., 2003). New strontium-isotope data from belemnites, brachiopods and oyster shells reported by Aurell et al. (in press) are coherent with the sedimentation of the Higueruelas Fm during the upper *A. eudoxus* zone and the *H. beckeri* zone (Fig. 1C).

The Higueruelas Fm is widely exposed south of Zaragoza (northeastern Spain, north Iberian Chain), in the outcrops located from the localities of Muel to Aguilón studied here (Fig. 2). The thickness of the unit ranges from 40 to 80 m in the east (i.e. basinward), reflecting a relatively homogeneous subsidence (e.g. Aurell et al., 2003). The boundaries of the Higueruelas Fm generally correspond to regional discontinuity

surfaces (Fig. 1D): the lower boundary is the contact with the underlying well-bedded (dm-scale) open-marine lime mudstone succession of the Loriguilla Fm (i.e. the boundary between the sequences Ki2 and Ki3); the upper boundary corresponds either to a basin-wide discontinuity (i.e. the upper boundary of the sequence Ki3) or to a boundary marked by the onset of coastal siliciclastic-dominated deposits in the more proximal, western logs studied in this work (e.g. Aguilón sector; Fig. 1D).

3. Studied successions and methodology

The 40 to 80 m-thick shallow-marine carbonate successions of the Higueruelas Fm were studied in 21 logs along the outcrops located south of Zaragoza (Fig. 2). The studied area is 20 x 30 km in extent, and the mean distance between logs is around 5 km. The studied sections are situated mainly on the flanks of E-W to NW-SE anticlines that developed during the Alpine compression (Cortés and Casas, 1996). The dip angle of the flank beds is generally low (10–30º, locally 80º in the localities of Tosos and Jaulín).

Facies analysis was based on both the bed-by-bed field descriptions of the 21 logs and the petrographic analysis of 1200 polished slabs and 300 thin sections. The description of texture was based on the Dunham (1962) classification. For the characterization of non-skeletal grains, the proposed nomenclatures for oncoids (Dahanayake, 1977, 1978), ooids (Strasser, 1986), and peloids (Flügel, 2004) were followed. The main characteristics of these non-skeletal grains are summarized in Table 1. The semi-quantitative proportion of skeletal and non-skeletal components in polished slabs and thin sections was ascertained by visual estimates using the comparison chart of percentages of constituents developed for limestones by Baccelle and Bosellini (1965).

Log correlation was carried out along three E-W-orientated (i.e. down-dip) cross-sections (Fig. 3). The lower datum for correlation is the sharp discontinuity surface between the thick-bedded (dm- to m-thick) limestones of the Higueruelas Fm (sequence Ki3) and the thin-bedded (dm-thick) lime mudstones of the underlying Loriguilla Fm (sequence Ki2; Fig. 1C) in the more proximal areas (i.e. studied sections in the localities of Muel, Jaulín, Mezalocha, Tosos and Aguilón). This discontinuity surface passes down dip (e.g. F1, F3 logs; Fig. 3) into a well-marked bedding surface within the uppermost Loriguilla Fm, which is coherent with the lateral relationship at basin-scale of the Higueruelas and Loriguilla formations (Bádenas and Aurell, 2001; Aurell et al., 2003). This implies that the boundary between the Higueruelas and Loriguilla formations is diachronous to the SE of the studied area. The analysis of the upper part of the Higueruelas Fm is locally prevented due to the erosive gap of variable amplitude and duration prior to the sedimentation of the overlying Cenozoic units (Fig. 3). In the more proximal areas (sections TO, A1, VH, MU and J1; Fig. 3), the uppermost part of the studied sequence Ki3 consists of the transition from carbonates to coastal siliciclastic-dominated facies (Ipas et al., 2007). In these proximal areas, therefore, the upper datum of the present study is the boundary between the Higueruelas Fm and these coastal facies, which is diachronous in the northwestern area (i.e. section MU) due to the earlier transition to siliciclastic deposits.

Well-marked bedding surfaces bounding nine sedimentary units were identified and correlated within the Higueruelas Fm in all the outcrops (1 to 9 in Figs 3 and 4). These are planar surfaces, some of which are

bioturbated or Fe-encrusted, and they occasionally correspond to hardgrounds. Locally cm-thick marly beds are associated with these surfaces. As no physical tracing between isolated outcrops of the Higueruelas Fm was possible (Fig. 2), log correlation was based on the best-fit correlation between these sharp bedding surfaces, also constrained by the vertical facies distribution observed in the successive sedimentary units defined in the individual logs. These sharp bedding surfaces are assumed to represent sedimentary discontinuities that can be traced across the entire studied area, and their correlation is supported by physical tracing along continuous outcrops (e.g. Mezalocha sector; Sequero et al., 2018). The km-scale lateral continuity of similar well-defined bedding surfaces has been demonstrated in other Kimmeridgian shallow carbonate ramp successions of the Iberian Basin (e.g. Bádenas and Aurell, 2010; Bádenas et al., 2010).

The sedimentary features of the facies, combined with their lateral and vertical relationships within the sedimentary units, were the key criteria for their palaeoenvironmental interpretation. Palaeogeographic maps were reconstructed for each sedimentary stage without palinspastic restoration, bearing in mind the low angle of the beds in the anticline flanks and the near absence of thrusts within the studied outcrops (Fig. 2).

4. Facies architecture

On the basis of texture, components and sedimentary structures, 19 facies were differentiated in the studied interval, representing deposition from inner- to mid-ramp areas. An example of their vertical distribution within the distinct sedimentary units is illustrated in Figure 4, and their lateral distribution is indicated in cross-sections in Figures 5 to 7. On the basis of their dominant components, the facies are grouped into three facies associations: peloidal and oolitic-dominated facies, oncolitic-dominated facies, and stromatoporoid/chaetetid/coral-rich facies. Their lateral relationships are identified by their detailed correlation within the sedimentary units between logs (see section 5). Facies descriptions are summarized below and illustrations of the different facies can be seen in Figures 8 to 12. Detailed information is included in Tables 1 to 3.

4.1. Peloidal and oolitic-dominated facies association

This association comprises 11 facies characterized by the predominance of peloids and ooids, and variable proportions of oncoids, intraclasts and bioclastic remains (Tables 2 and 3). These facies represent intertidal areas (i.e. peloidal mudstone to packstone-grainstone with fenestral porosity), restricted lagoon areas (peloidal-bioclastic-type 3 and 4 ooid wackestone to grainstone), backshoal areas (peloidal-type 1 and 1/3 ooid wackestone to grainstone, and bioturbated peloidal packstone to grainstone) and shoal-sand blankets (peloidal to oolitic grainstone facies) on the inner ramp, to foreshoal (peloidal wackestone-packstone to grainstone), offshore-proximal (peloidal-bioclastic wackestone to packstone) and offshore-distal areas (bioclastic-peloidal mudstone) on the middle ramp. The lateral relationship of intertidal, lagoon and backshoal facies can be seen in sedimentary units 5 to 7 (Figs 5 to 7). The lateral relationship

of backshoal, shoal-sand blanket, foreshoal and offshore facies is evident in most of the units (e.g. units 1 and 2 in Fig. 7; units 2 and 3 in Fig. 5).

Peloidal mudstone (M) to packstone-grainstone (P-G) with fenestral porosity is characterized by the predominance of lithic peloids, and a lower proportion of type 1 and 1/3 ooids (Strasser, 1986), type II oncoids (Dahanayake, 1977) (Table 1), and skeletal grains (mainly of lituolids, miliolids, texturaliids, bivalves and *Tubiphytes-Crescentiella*; Fig. 8a). Fenestral porosity indicates the trapping of air bubbles in the sediment by turbulent flows related to waves, algal growth and decay, or desiccation and the rapid precipitation of cements (e.g. Shinn, 1968; Flügel, 2004). The presence of *Girvanella* and *Bacinella* growths and dome-like stromatolitic structures indicates sediment trapping by microbial mats in intertidal areas. Facies correlation indicates that these mud-supported and grain-supported sediments represent a continuous intertidal belt located to the northwest (Figs 5 and 6) and local tidal caps on grain-supported deposits (e.g. peloidal-oolitic shoal-sand blankets and washover deposits in sections TO and J3, respectively, Figs 5 and 7; see also Sequero et al., 2018).

Peloidal-bioclastic-type 3 and 4 ooid wackestone (W) to grainstone (G) occurs in the upper part of the succession (Figs 5 to 7). It is composed of well-sorted and rounded lithic peloids, radial type 3 and 4 ooids (Strasser, 1986) and highly micritized or ferruginous bioclasts (mainly bivalves, lituolids, gastropods, ostracods and echinoderms; Fig. 8b, c). The facies shows frequent bioturbation (*Thalassinoides* traces) and cm-thick bioclastic laminae with normal gradation and parallel lamination. The observed features indicate alternating low-energy conditions (burrowing and micritization of skeletal grains) and moderate-energy conditions (lithic peloids, radial type 3 and 4 ooids, cm-thick bioclastic laminae). Deposition probably took place in a restricted lagoon, as indicated by the low diversity of the skeletal remains. Some intercalated marls indicate periods of higher detrital input.

Peloidal-type 1 and 1/3 ooid W to G and bioturbated peloidal P to G facies represent the backshoal/washover peloidal-oolitic facies. The peloidal-oolitic W to G has abundant lithic peloids, and variable proportions of ooids, oncoids and skeletal grains (Fig. 8d-f). Compound and aggregate grains are common, and the main skeletal grains are foraminifera (lituolids, miliolids, textulariids), brachiopods, bivalves, echinoderms, gastropods and dasycladacean algae. The facies shows a mixture of components derived from the laterally related facies, e.g. protected-marine fauna (i.e. dasycladacean algae; Fig. 8e) similar to the lagoon facies, and type 1 and 1/3 ooids and oncoids similar to those of the shoal-sand blanket facies. This mixture of components, and the presence of aggregate grains, bioturbation, parallel and cross-lamination, and mm- to cm-thick oncolitic, skeletal and oolitic laminae with normal gradation, indicate that this facies corresponds to washover deposits as well as backshoal sediments (e.g. Bádenas and Aurell, 2010). Bioturbated peloidal P to G occurs at the top of the succession, also laterally related to restricted lagoon and peloidal shoal-sand blanket facies (e.g. unit 5 in Fig. 5; and unit 8 in Fig. 6). The predominance of well-sorted lithic peloids (Fig. 8g), micritized skeletal grains (mainly lituolids, miliolids, gastropods, echinoderms and bivalves), and intense burrowing (*Thalassinoides* traces) reflect accumulation in a backshoal subenvironment close to the peloidal shoal-sand blankets.

The peloidal to oolitic grainstone facies include three types of facies, each one characterized by the predominance of specific non-skeletal grains (Fig. 9a-c): peloidal G with well-sorted and rounded lithic

peloids (Fig. 9a) and a lesser proportion of type 1 and 1/3 ooids and type IV oncoids; type 1 and 1/3 ooid-peloidal G, with a similar percentage of lithic peloids and type 1 and 1/3 ooids (Fig. 9b); and type 1 and 1/3 ooid G, dominated by smaller (up to 0.5 mm-sized) and well-sorted type 1 and 1/3 ooids (Fig. 9c). The grainstone texture, the predominance of high-energy ooids (type 1 and 1/3 ooids) and lithic peloids, and the scarce skeletal content reflect the continuous agitation of shoal-sand blankets above the fair-weather wave base (i.e. inner ramp). Despite the absence of cross-bedding, frequent local tidal caps on these facies (e.g. sections TO and F5 in Fig. 7) reflect a certain relief above the sea bottom.

Peloidal W-P to G has similar components and structures (common bioturbation, local parallel lamination) to those described in peloidal to oolitic shoal-sand blankets. It includes mainly lithic peloids and type 1 and 1/3 ooids (Fig. 9d), although this facies has a higher matrix and skeletal content (mainly lituolids, miliolids, echinoderms, brachiopods and bivalves). These characteristics and its lateral relationship with shoal-sand blanket and offshore facies (Figs 5 to 7) indicate deposition in the foreshoal subenvironment, below the fair-weather wave base.

The peloidal-bioclastic W to P and bioclastic-peloidal M facies developed down-dip of the foreshoal facies (Figs 5 to 7) and reflect a progressive loss of non-skeletal grains from shallow areas. The peloidal-bioclastic W to P is mainly formed by lithic and local microbial peloids (Fig. 9e; Table 1), with a lower proportion of oncoids (type II and IV oncoids with thick crusts of *Bacinella* and *Girvanella*) and a skeletal content characteristic of open-marine areas, including some belemnites (Tables 2 and 3). The intercalation with foreshoal and mud-dominated offshore facies, frequent bioturbation (*Chondrites* and *Planolites* traces) and an open-marine faunal association indicate deposition in an offshore-proximal subenvironment with generally low energy. The bioclastic-peloidal M has scarce lithic peloids and type I and II oncoids, as well as open-marine skeletal grains (Fig. 9f). These characteristics, the frequent bioturbation and its lateral relationship with offshore-proximal facies indicate deposition in a low-energy offshore-distal subenvironment. The scarce type I and II oncoids were probably resedimented from proximal areas during storms.

One particular facies, intraclastic-peloidal P to G, appears in the upper part of the succession, laterally related to various facies, mainly backshoal/washover to foreshoal facies (e.g. unit 6; Figs 5 and 6). The intraclastic-peloidal facies occurs as isolated dm-thick beds, with components accumulated in mm- to cm-thick laminae. The limited lateral extent of this facies obtained from the correlation, combined with the predominance of lithic peloids and mm- to cm-sized intraclasts of mud- and grain-supported facies (Fig. 8h; Table 2), indicates that this facies would correspond to storm lobes in both backshoal and foreshoal subenvironments, with resedimented intraclasts derived from lateral mud- and grain-supported facies.

4.2. Oncolitic-dominated facies association

This association comprises four facies characterized by an abundance of oncoids, formed in pond/restricted lagoon, sheltered lagoon, backshoal, shoal-sand blanket to foreshoal subenvironments (Figs 5 to 7; Tables 2 and 3). Sheltered lagoon facies (type IV oncoid W to P) and pond/restricted lagoon facies (gastropod-oncolitic W-P to G) are only present in the northwestern area in sedimentary units 3 and

5, respectively (section ME1; Fig. 6). The pond/restricted lagoon gastropod-oncolitic facies is laterally related to restricted peloidal-bioclastic-oolitic-dominated lagoon and peloidal-dominated fenestral facies (see also the facies correlation in this area by Sequero et al., 2018). The sheltered lagoon oncolitic facies is laterally associated with the peloidal-oolitic backshoal facies, and grades laterally into the backshoal to foreshoal oncolitic-dominated facies (type III oncoid P, and type II and III oncoid G; e.g. sedimentary units 1-4 and 8; Figs 5 to 7).

Gastropod-oncolitic W-P to G is characterized by an abundance of broken and whole gastropods, and type I, II and IV oncoids (Fig. 10a), and has variable proportions of lithic peloids, type 1 and 1/3 ooids and small, commonly micritized skeletal grains (mainly of bivalves, lituolids, miliolids and textulariids). The predominance of gastropods, the presence of non-skeletal components similar to the laterally related fenestral facies, and the intercalation of marls indicate deposition in a restricted lagoon or in ponds within the intertidal area. Components that accumulated in cm-thick laminae reflect high-energy events, probably storms.

Type IV oncoid W to P has abundant irregular type IV oncoids (up to 7 cm in size), with bioclastic cores and thick crusts composed of a meshwork of cyanobacteria (mainly *Bacinella-Lithocodium*) (Fig. 10b, c). Type III oncoids are also common. The oncoids are surrounded by a fine-grain-sized fraction composed of lithic peloids and skeletal grains (mainly micritized lituolids, miliolids, textulariids, bivalves, echinoderms and brachiopods). The predominance of type IV oncoids, bioturbation and micritized skeletal grains reflect deposition in a sheltered, low-energy lagoon. Type III oncoids suggest short, higher-energy periods favouring the generation of micritic laminae (e.g. Dahanayake, 1977). Small micritic oncoids, ooids and intraclasts were resedimented from the laterally related facies, mainly from the peloidal-oolitic backshoal/washover facies.

Type III oncoid P comprises 20 to 60% oncoids, in some cases forming oncolitic-supported textures (Fig. 10d-f). This facies has abundant type III oncoids (up to 2 cm in size), with bioclastic and intraclastic cores, and alternating micritic laminae and organism-bearing encrustations, mostly of *Bacinella-Lithocodium* (Fig. 10f). Type II, IV and compound oncoids are common, and the fine-grain-sized fraction is composed of peloids (lithic and microbial peloids), type 1 and 1/3 ooids and skeletal grains (lituolids, miliolids, textulariids, echinoderms, gastropods, bivalves, brachiopods, stromatoporoids and chaetetids). The abundance of type III oncoids suggests alternating higher- and lower-energy conditions, the latter favourable for microbial growth. The lateral facies relationships indicate that this facies occurs in the backshoal and foreshoal subenvironments (e.g. units 1-2 in Figs 6 and 7).

Type II and III oncoid G, which has similar proportions of oncoids to type III oncoid P, is characterized by an abundance of type II and III oncoids (up to 2 cm in size), with bioclastic and intraclastic cores, thick micritic laminae and a minor development of organism-bearing encrustations (mainly *Bacinella*) (Fig. 10g). Type I and compound oncoids are also common, and the fine-grain-sized fraction is composed of lithic peloids, type 1 and 1/3 ooids and skeletal grains (lituolids, echinoderms, bivalves and brachiopods). The grainstone texture, the abundance of type II and III oncoids and the lateral facies associations indicate that this facies occurs in the shoal-sand blanket subenvironment (e.g. units 1-2 in Figs 5 and 7).

4.3. Stromatoporoid/chaetetid/coral-rich facies association

This association is characterized by an abundance of stromatoporoids, chaetetids and corals, and includes four facies: stromatoporoid W to G and oncolitic-stromatoporoid W to G in lagoon to backshoal areas; and chaetetid-stromatoporoid-coral buildups and laterally associated stromatoporoid-chaetetid-coral and oncolitic W to G, which developed in mid-ramp foreshoal to offshore-proximal areas (Figs 5 to 7; Tables 2 and 3). The lateral relationship of these facies has been characterized in most of the units (e.g. units 2-5 in Fig. 7). The stromatoporoid W to G and oncolitic-stromatoporoid W to G facies are laterally associated with oncolitic-dominated and peloidal and oolitic-dominated lagoon and backshoal facies, respectively. The chaetetid-stromatoporoid-coral buildups and stromatoporoid-chaetetid-coral and oncolitic W to G facies are laterally associated with peloidal and peloidal and bioclastic-dominated foreshoal and offshore-proximal facies, respectively, and locally with oncolitic-dominated foreshoal facies.

The stromatoporoid W to G has abundant broken and in-situ stromatoporoids (mainly *Cladocoropsis*), and cm-sized fragments of chaetetids and corals, both with *Tubiphytes-Crescentiella* encrustations and bivalve borings (Fig. 11a, b). Local cm-sized domal growth forms of stromatoporoids are recognized. The fine-grain-sized fraction is mainly composed of peloids (lithic and microbial peloids; Fig. 11c) and small skeletal grains (mainly bivalves, brachiopods, echinoderms, lituolids, miliolids, texturaliids and dasycladacean algae). The oncolitic-stromatoporoid W to G has abundant oncoids (mainly type II and IV) and stromatoporoid, chaetetid and coral fragments (Fig. 11d). The fine-grain-sized fraction is mainly composed of peloids (lithic and microbial peloids) and small skeletal grains (mainly debris of *Tubiphytes-Crescentiella*, lituolids, miliolids, textulariids, bivalves, gastropods, echinoderms and brachiopods). Bioturbation and mm- to cm-thick accumulations of coarse grains are also common.

The stromatoporoid W to G and lateral oncolitic-stromatoporoid W to G represent stromatoporoid carpets in lagoon to backshoal areas. The term “carpet” refers to densely spaced stromatoporoid colonies that do not create a distinctly three-dimensional structure, but form relatively thin veneers of colonial organisms following the existing sea-floor morphology (e.g. Riegl and Piller, 2000). The facies mapping in the Mezalocha outcrops (Fig. 6) reflects the fact that these carpets did not develop in the entire lagoon but formed patches, locally more than 500 m in lateral extent (Sequero et al., 2018). The oncolitic-stromatoporoid W to G corresponds to sediment surrounding the stromatoporoid carpets (Figs 5 to 7; see also Sequero et al., 2018), as indicated by their lateral relationship and the similarity of the components in these two facies (Table 2 and 3). The common presence of stromatoporoids in lagoonal settings has been highlighted by previous authors (e.g. Flügel, 1974; Turnsek et al., 1981; Leinfelder et al., 2005; Aurell et al., 2012; San Miguel et al., 2017a). The predominance of stromatoporoids over corals was probably due to moderate water-energy, oligotrophic conditions in the lagoon and backshoal subenvironments (e.g. Leinfelder et al., 2005). The presence in the fine-grain-sized fraction of peloids, bivalves, echinoderms, foraminifera, dasycladacean algae, *Thaumatoporella* and *Cayeuxia-Ortonella* (Tables 2 and 3) indicates well-oxygenated, normal-marine waters.

The chaetetid-stromatoporoid-coral buildups have a lenticular geometry up to 8 m high and around 250 m wide (i.e. section F5; Fig. 12; Bádenas and Aurell, 2003). The reef fabric consists of chaetetids (e.g. *Ptychochaetetes*, *Blastochaetetes*; Tables 2 and 3) and less abundant stromatoporoids and corals (Fig. 11e, f), surrounded by micritic to peloidal microbial crusts with encrusting organisms (serpulids, foraminifera, sponges, *Cayeuxia-Ortonella*, *Thaumatoporella*, *Lithocodium*, *Bacinella*, *Girvanella*, *Troglotella*; Bádenas and Aurell, 2003). The internal structure is similar to those observed in the so-called disrupted frame reefs defined by Riding (2002), where broken and weakly eroded colonial organisms constitute the three-dimensional structure. The fine-grain-sized fraction recognized in internal cavities (a few mm to cm in size) is mainly composed of microbial peloids, small skeletal grains (mainly brachiopods, bivalves, echinoderms, serpulids, *Cayeuxia-Ortonella* and sponges), microbial crust fragments and oncoids (mainly type I and II). Bivalve and sponge borings are also found. The stromatoporoid-chaetetid-coral and oncolitic W to G, which is laterally related to these buildups, is characterized by cm-sized fragments of stromatoporoids, chaetetids and corals with variable proportions of oncoids (type II, III and IV) (Fig. 11g, h). The fine-grain-sized fraction is composed of microbial and lithic peloids, and mm- to cm-sized echinoderms, bivalves, brachiopods and gastropods. Bivalve and serpulid borings on stromatoporoids and chaetetids are also common.

The buildups developed in the foreshoal and offshore-proximal subenvironments, below the fair-weather wave base within the photic zone, as indicated by the presence of light-dependent organisms (e.g. *Cayeuxia-Ortonella*, *Girvanella*, *Bacinella*, *Thaumatoporella*) and their intercalation within foreshoal to offshore-proximal peloidal and peloidal-bioclastic facies (Figs 5 to 7; Tables 2 and 3). The stromatoporoid-chaetetid-coral and oncolitic W to G represents inter-buildup sediment, as indicated by its lateral relationship with the chaetetid-stromatoporoid-coral buildups (Figs 5 to 7) and the similarity of the components in these two facies (Table 2 and 3). The cm-sized fragments of stromatoporoids, chaetetids and corals resulted from the destruction and reworking of the buildups, whereas oncoids are formed in-situ.

5. Facies evolution and sedimentary models

The facies distribution observed throughout the nine sedimentary units allowed the spatial distribution of the facies to be determined, showing their variable extent and the complexity in their lateral (along strike and down-dip) relationships (Figs 13 and 14). On the basis of the relative abundance of specific facies and their spatial distribution, two facies models are proposed: an oncolitic-peloidal-oolitic-dominated ramp, encompassing sedimentary units 1 to 4, and an oolitic-peloidal-dominated ramp, in sedimentary units 5 to 9 (Fig. 15). The down-dip gradation of the main non-skeletal grains in these two models is indicated in the simplified sedimentary models of Figure 16.

5.1. Oncolitic-peloidal-oolitic-dominated ramp

This sedimentary model corresponds to sedimentary units 1 to 4 (Figs 13 and 15A) and is mainly characterized by: (1) the relative abundance of oncolitic-dominated facies from backshoal to foreshoal subenvironments, (2) the development of a low-energy oncolitic sheltered lagoon, and (3) the growth of stromatoporoid carpets in backshoal/washover areas.

Peloidal-oolitic shoal-sand blankets dominate, with a general north-to-south orientation of the facies belt. Laterally (along strike), oncolitic shoal-sand blankets (type II and III oncoid G) are also present. In particular, the widest record of oncolitic-dominated shoal-sand blankets is found in sedimentary unit 1 (Fig. 13A), passing laterally (along strike) to peloidal-oolitic shoals (type 1 and 1/3 ooid-peloidal G) and laterally (down dip) to oncolitic backshoal and foreshoal (type III oncoid P) facies. The foreshoal domain is peloidal-dominated (peloidal W-P to G) and passes down dip (to the SE) to peloidal-bioclastic offshore-proximal and offshore-distal facies. Chaetetid-stromatoporoid-coral buildup and inter-buildup facies occur in the foreshoal and offshore-proximal subenvironments, with a patchy distribution (from 2 km to up to 10 km in width).

The onset of sedimentary unit 2 is marked by the progradation of the shoal-sand blanket eastward (Fig. 13B), and the first appearance of intertidal domains and stromatoporoid carpets in the backshoal area dominated by peloidal-oolitic sediments (peloidal-type 1 and 1/3 ooid W to G facies). Peloidal and lateral (along strike) oncolitic shoal-sand blankets developed with a down-dip extension of around 5 km and with local intertidal patches on top. Facies in the foreshoal and offshore subenvironments are similar to stage 1, but the offshore-proximal area is twice as wide in stage 2 (around 10 km) as in stage 1.

A low-energy oncolitic sheltered lagoon develops in sedimentary unit 3 (Fig. 13C), laterally (down dip) in relation to the peloidal-oolitic backshoal/washover facies (peloidal-type 1 and 1/3 ooid W to G). An intertidal belt is recognized in the northwestern sector, laterally to the peloidal-oolitic backshoal of stages 2-4. Stromatoporoid-rich carpets grew in the backshoal area within peloidal-oolitic backshoal sediments and oncolitic backshoal sediments (type III oncoid P), with a patchy distribution (500 m in lateral extent). Peloidal-oolitic shoal-sand blankets (type 1 and 1/3 ooid-peloidal G) with local intertidal patches predominate, although locally (along strike) type II and III oncoid shoals are recognized (around section J1; Fig. 13C). The shoal-sand blankets in sedimentary unit 3 are of a similar down-dip extension to those in unit 2 but they prograde eastward in unit 3. In unit 4, this high-energy facies belt has a wider down-dip extension (up to 12 km; Fig. 13D). Chaetetid-stromatoporoid-coral buildups grew in the offshore-proximal subenvironment, with a similar patchy distribution and extension (up to 10 km) to those in stages 1 to 2.

In summary, the resulting oncolitic-peloidal-oolitic-dominated ramp shows a down-dip (NW-SE) succession of facies belts, but also some mosaic facies of variable extension (Fig. 15A): intertidal belt (at least 3 km in down-dip extension); local sheltered lagoon; backshoal/washover (3 to 8 km in down-dip extension) with a mosaic of stromatoporoid carpets and related oncolitic sediments (patches of 500 m in width); shoal-sand blanket (3-12 km in down-dip extension) with local intertidal caps (less than 3 km in diameter) on top; and foreshoal (2-7 km) and offshore domains (3-10 km in the offshore-proximal subenvironment), with patches of chaetetid-stromatoporoid-coral buildup and inter-buildup facies (from 2 km to up to 10 km in diameter). Lithic peloids, type 1 and 1/3 ooids, and type II, III and IV oncoids are

the main non-skeletal grains, especially in the inner ramp (Fig. 16A): peloids characterize the intertidal domain; low-energy conditions in the sheltered lagoon determined the abundance of type IV oncoids; the backshoal/washover, shoal-sand blanket and foreshoal subenvironments are mainly composed of peloids and type 1 and 1/3 ooids, with lateral (along strike) areas where type II and/or III oncoids predominate. These components decrease in abundance down dip, especially in the offshore-distal subenvironment, where only scarce peloids and type I and II oncoids are found. As regards metazoans, stromatoporoids predominate in backshoal and sheltered lagoon areas, whereas chaetetid-stromatoporoid-coral associations predominate in buildup and inter-buildup facies in the foreshoal and offshore-proximal subenvironments, below the fair-weather wave base.

5.2. Oolitic-peloidal-dominated ramp

The oolitic-peloidal-dominated ramp corresponds to sedimentary units 5 to 9 (Figs 14 and 15B), and is mainly characterized by: (1) the widespread development of a restricted lagoon, (2) the predominance of peloidal shoal-sand blankets, and (3) the occurrence of intraclastic-peloidal storm lobes in backshoal and foreshoal areas.

Sedimentary unit 5 reflects the development of a wide peloidal-bioclastic-oolitic restricted lagoon (peloidal-bioclastic-type 3 and 4 ooid W to G), with a down-dip extension of around 10 km, locally grading onshore into the intertidal domain with local ponds (gastropod-oncolitic W-P to G; Fig. 14A). The backshoal area is peloidal-oolitic and intraclastic-dominated (peloidal-type 1 and 1/3 ooid W to G and intraclastic-peloidal P to G), the latter related to storm lobes (2-7 km in width). The sheltered lagoon and stromatoporoid carpets present in the previous stage have disappeared; only very local stromatoporoid carpets are found in the backshoal area in sedimentary unit 6 (i.e. section J2; Fig. 14B). The shoal-sand blankets are mainly composed of peloids, with significant variations in lateral extent (from 4 to 11 km), as observed in the previous stage. Local intertidal caps (1-5 km in width) are observed on top of the backshoal/washover and shoal-sand blanket deposits. Also local intraclastic-peloidal storm lobes occur in the foreshoal subenvironment. Chaetetid-stromatoporoid-coral buildup and inter-buildup facies developed in the foreshoal and offshore-proximal subenvironments, with a similar patchy distribution and extension to the previous stage (2 to 7 km). Oncolitic-dominated backshoal, shoal-sand blanket and foreshoal facies are considerably reduced, occurring only locally in sedimentary units 5, 6 and 8. Bioturbated peloidal P to G backshoal facies occurs in sedimentary units 7 and 8 (Fig. 14C, D), being widely developed in sedimentary unit 8 (10 km in lateral extent) and grading down dip into peloidal shoal-sand blanket and peloidal-oolitic backshoal facies. As a whole, there is a progressive progradation of shallow facies to the east and an increase in siliciclastic input in shallower areas (i.e. coastal siliciclastic-dominated deposits; Figs 3 and 14C-E).

There is no stratigraphic record of carbonate shallow-marine facies belts in most of the sections for sedimentary unit 9, except local intertidal and oncolitic-dominated facies (Fig. 14E).

In summary, the facies distribution observed in this oolitic-peloidal-dominated ramp shows the down-dip gradation of peloidal-dominated intertidal belt, restricted lagoon (around 10 km wide),

backshoal/washover (2-12 km in lateral extent), shoal-sand blanket (4-11 km in width), foreshoal (2-7 km wide) and offshore-proximal subenvironments, with local oncolitic-dominated facies in intertidal/restricted lagoon (i.e. local ponds in the intertidal belt or restricted lagoon; around 2 km wide), backshoal and foreshoal areas (2-3 km in down-dip extent), storm lobes (2-7 km in width) in backshoal and foreshoal domains, and local intertidal caps (1-5 km in diameter) on top of backshoal and shoal-sand blanket deposits (Fig. 15B). Peloids constitute the main non-skeletal component from inner- to mid-ramp domains, as well as type 3 and 4 ooids in the restricted lagoon and a minor proportion of type 1 and 1/3 ooids from intertidal to backshoal and foreshoal subenvironments (Fig. 16B). Intraclasts are also abundant in storm-related lobes, mostly occurring in the backshoal area, as well as type III oncoids especially in the foreshoal area. Intense local burrowing takes place in peloidal-dominated backshoal deposits, laterally related to the peloidal shoal-sand blankets. As regards the stromatoporoid/chaetetid/coral-rich facies, only chaetetid-stromatoporoid-coral buildup and inter-buildup facies are maintained from the foreshoal to offshore-proximal subenvironments. The stromatoporoid carpets in the lagoon and backshoal have disappeared.

At a long-term scale, the sedimentary evolution of the carbonate ramp throughout the nine sedimentary units reflects a shallowing-upward trend, with the progradation of the inner ramp facies towards the east-southeast.

6. Discussion

6.1. Factors controlling facies distribution

The facies heterogeneity and sedimentary evolution observed throughout the nine sedimentary units reflect the combined role of internal processes and external factors. Long- to short-term variations in accommodation space related to sea-level fluctuations, along with irregular bottom topography, water transparency and water energy conditioned the spatial distribution and lateral continuity of the facies (e.g. Kerans and Tinker, 1997; Della Porta et al., 2002; Hillgärtner, 2006).

The spatial distribution of the shoal-sand blankets determined the nature of the laterally related inner ramp and mid-ramp facies. The shoal-sand blankets show a general N-S orientation, with significant differences in their lateral extent (i.e. from 3 to 12 km; Figs 13 and 14). They are mainly composed of peloidal and oolitic G (type 1 ooid with micritic laminae or type 1/3 with alternating micritic and sparitic laminae), which grades laterally (along strike) into oncolitic G (type II and III oncoids), with peloids and ooids in similar measure in the fine-grain-sized fraction. Lithic peloids and ooids found in the peloidal to oolitic G facies represent continued high-energy conditions (Strasser, 1986) compared to the type II and III oncoid G facies, which reflects lower water agitation since these oncoids are partially composed of organism-bearing encrustations (Dahanayake, 1977). Certain sectors of the shoal-sand blankets are partially or completely represented by the oncolitic-dominated facies. These along-strike variations in non-skeletal grains were probably controlled by the irregular topography of the shoal-sand blanket belt, with possible depressions/protected areas where lower water energy favoured the generation of type II

and III oncoids. Differences in depositional topography are also highlighted by the presence of intertidal caps on top of peloidal-oolitic shoal-sand blankets, but not on the oncolitic shoal facies. The shoal-sand blankets show a similar N-S orientation throughout the nine sedimentary units, but vary in their lateral extent (from 3 to 12 km). This belt could have been controlled by wave energy, which redistributed the sediment especially during storms (e.g. Reijmer et al., 2009). The prevailing NE-SW direction of winter winds and the SE-NW direction of the hurricane pathways affecting the Iberian Basin (Marsaglia and Klein, 1983; Golonka et al., 1994; Price et al., 1995; Fig. 1B) suggest that longshore currents possibly controlled the N-S orientation of this facies belt, and that storm resedimentation determined the variations in down-dip lateral extension. The influence of storms on this carbonate ramp is highlighted by the recurrence of storm-related intraclastic-peloidal lobes in both backshoal and foreshoal subenvironments, especially in the oolitic-peloidal-dominated ramp (see sedimentary units 5 to 7 in Fig. 14).

Offshore from the shoal-sand blanket, a gradation of sediments composed of peloids, ooids, oncoids and bioclasts is observed, from foreshoal peloidal W-P to G, to offshore-distal bioclastic-peloidal M. This is related to the down-dip decrease in water energy. The open-marine areas are favourable for the growth of chaetetid-stromatoporoid-coral buildups, below the fair-weather wave base. The presence of these suspension-feeding metazoans and light-dependent micro-encrusters reflects low- to moderate water energy, water transparency and oligotrophic conditions (Leinfelder et al., 1993). Local heterogeneities in the distribution of some non-skeletal grains are found in the inter-buildup facies, some of which is dominated by in-situ-generated oncoids with organism-bearing encrustations (i.e. type II, III and IV oncoids). The preferential growth of these buildups and inter-buildup oncolitic sediments in some areas of the foreshoal and offshore-proximal subenvironments is open to interpretation. It could be related to areas where storms remobilized unconsolidated sediment and left the underlying hard substrate exposed and available for colonization by metazoans.

In the earlier stage of evolution (sedimentary units 1 to 4), an oncolitic-peloidal-oolitic-dominated ramp developed, with a local sheltered lagoon characterized by an abundance of large and irregular type IV oncoids (Figs 13 and 15A). The shoal-sand blankets acted as a barrier to water energy and favoured the generation of low-energy conditions for bacterial growth. Low-energy conditions, negligible siliciclastic input and possible low sedimentation rates contributed to the extensive growth of oncoids with light-dependent and oligotrophic micro-encrusters (e.g. Leinfelder et al., 1993; Dupraz and Strasser, 1999). The reduced lateral extent of this lagoon was conditioned by the sediment reworked in the backshoal area and by storm-induced flows (i.e. washover deposits), which led to abrupt changes in facies distribution by redistributing sediment in large quantities (Strasser and Védrine, 2009). Stromatoporoid-rich carpets occurred within the sheltered lagoon and backshoal subenvironments, where the bioclastic association also indicates good water transparency and oligotrophic conditions. On the basis of a detailed sedimentological study in the northwestern area (i.e. around the locality of Mezalocha; see Fig. 2) by Sequero et al. (2018), it was suggested that the preferential growth of these stromatoporoid-rich carpets within the lagoon and backshoal/washover subenvironments was probably related with the presence of local hard substrates and areas with higher-energy conditions that occurred in corridors created between washover deposits.

The oolitic-peloidal-dominated ramp in units 5-9 (Figs 14 and 15B) reflects the predominance of peloids and ooids to the detriment of oncoids. Restricted conditions characterize the inner ramp lagoon (peloidal-bioclastic-type 3 and 4 ooid W to G) with a minor development of oncolitic ponds (gastropod-oncolitic W-P to G) compared with the previous stage. Peloidal-dominated facies are widely developed from the lagoon to offshore-proximal subenvironments. The relative abundance of peloidal facies at this stage in the evolution of the platform, together with the near disappearance of stromatoporoid-rich carpets in the lagoon and backshoal, point to an increase in water energy and/or fluctuations in salinity conditions that would not have been favourable for microbial activity and the growth of stromatoporoids, chaetetids and corals. A lateral siliciclastic-dominated unit is recorded in unit 7 in the northwestern area (Fig. 14C), suggesting an increased terrigenous input to the lagoon carbonates. General lower-energy conditions were established in the backshoal subenvironment during the deposition of sedimentary unit 8 (Fig. 14D), as indicated by the intense burrowing and the absence of storm-related deposits.

As a whole, the observed facies distribution can be related to long- to short-term sea-level fluctuations. The progressive progradation of the shallow facies belts (Figs 13 and 14) is likely to be associated with the long-term fall in sea level occurring at the end of the Jurassic in the Iberian Basin (Salas et al., 2001; Aurell et al., 2003, 2010). The decrease in accommodation space would have controlled aspects such as the generation of more restricted conditions in the inner ramp, as the connection with the open-marine areas was reduced, and the local subaerial exposure of both backshoal and shoal-sand blanket deposits.

The internal processes occurring in this carbonate ramp, which in great measure determine the distribution and lateral migration of the facies, may also overprint possible environmental changes induced by insolation variations in the Milankovitch frequency band (e.g. Strasser, 2018). The influence of orbitally-induced cycles on the sedimentation of Jurassic Iberian platforms has previously been documented in Kimmeridgian-Tithonian shallow to deeper marine carbonate successions (e.g. Bádenas et al., 2004, 2005). In particular in the shallow areas of the carbonate ramp, the influence of sea-level fluctuations related to short-term eccentricity cycles resulted in the formation of high-frequency sequences bounded by discontinuity surfaces that can be physically traced at km-scale (Bádenas and Aurell, 2010, 2018). According to the lateral continuity assumed here for the well-marked bedding surfaces, the nine sedimentary units differentiated within the Higueruelas Fm (Fig. 3) could represent high-frequency sequences linked to high-order sea-level fluctuations. Examples of sedimentary trends in the high-frequency sequences and their bounding surfaces are shown in Figure 17. Most of the sequence boundaries are planar bedding surfaces, locally bioturbated surfaces (e.g. between sequences 5 and 6 in section V), hardgrounds (e.g. between sequences 1 and 2 in section J2) or are associated with cm-thick marly beds (e.g. between sequences 2 and 3 in section MU). The vertical facies trend within the sequences is variable (aggradational, shallowing, deepening and locally deepening-shallowing), and in a single correlated high-frequency sequence can vary from log to log. For instance, sequence 2 displays a shallowing trend in more proximal areas (i.e. section MU), but a deepening or aggradational trend in distal areas (i.e. sections J3 and V). The presence of well-marked high-frequency sequence boundaries, but not of maximum flooding surfaces, fits well with their development in a long-term regressive stage, whereas marked maximum flooding surfaces in high-frequency sequences would tend to be recorded during the maximum flooding intervals of long-term sequences (Strasser et al., 1999). Judging by the

number of sequences (i.e. nine sedimentary units) and by the time span of the sequence Ki3 in the central part of the Iberian Basin as obtained by biostratigraphic data (ammonites, larger benthic foraminifera) and strontium-isotope data (around 1.2 Myr; Aurell et al., in press), the estimated duration for each sequence is around 133 ky, thus falling within the range of short-term eccentricity orbital cycles (ca. 100 ky).

6.2. Lateral continuity of grain-supported facies: implications for reservoir exploration

A knowledge of the lateral continuity of facies belts and their stacking patterns in outcrop analogues of carbonate reservoirs is important in assessing the dimensions of potential reservoir-rock bodies on the basis of subsurface data. Most of the facies that characterize the Higueruelas Fm are similar to those found in the Arab-D Formation, the major hydrocarbon carbonate reservoir in the Middle East (Al-Awwad and Collins, 2013). As in the analogue Higueruelas Fm, the deposits of the Arab-D Fm occurred in the shallow domains of an upper Kimmeridgian carbonate ramp (Ayoub and En Nadi, 2000; Al-Saad and Ibrahim, 2005), and the more productive facies generally consist of well-sorted oolitic packstone-grainstones forming active shoals and patch buildups mainly composed of stromatoporoids in the foreshoal subenvironment (Grötsch et al., 2003). The quality of many of these reservoirs is due to the interparticle porosity in the peloidal and oolitic grainstones, and the vuggy porosity resulting from the dissolution of stromatoporoid bioclasts (Wender et al., 1998; Gröstch et al., 2003; Hughes, 2004; Lindsay et al., 2006).

A gradation of grain-supported facies from intertidal to foreshoal subenvironments has been characterized in the Higueruelas Fm. Grain-supported peloidal-oolitic and oncolitic-dominated facies characterize the backshoal, shoal-sand blanket and foreshoal domains, which also include stromatoporoid-rich carpets and chaetetid-stromatoporoid-coral buildup and inter-buildup facies in inner- and mid-ramp areas, respectively. Packstone-grainstone and grainstone textures from these facies are highlighted in Figure 18, in order to reveal the dimension and lateral continuity of potential analogue carbonate reservoir-rock bodies in the Higueruelas Fm.

Grainstone textures are mostly recorded in the shoal-sand blankets, laterally related to backshoal and foreshoal grainstone facies (Figs 5 to 7) grading locally into packstone-grainstone textures. Lateral continuity is observed for these grainstone bodies, as is their great down-dip extent, especially in sedimentary units 2, 4 and 5 (Figs 13 and 14). Stromatoporoid carpets developed in packstone-grainstone and grainstone backshoal deposits in sedimentary units 2, 3 and 6, whereas stromatoporoid buildups and inter-buildup facies occurred in packstone-grainstone foreshoal sediments in units 1, 2, 6 and 7 (Fig. 18). This spotlights an additional interest in these backshoal and foreshoal deposits, since vuggy porosity resulting from the dissolution of stromatoporoid bioclasts is another major reservoir-improving factor.

Characterization of the dimension and lateral continuity of potential carbonate reservoir-rock bodies in outcrop analogues is essential for hydrocarbon exploration, but so are the barriers (i.e. continuous low-permeability layers) that compartmentalize the reservoir field, which usually correspond to mud-supported sedimentary facies or highly cemented deposits caused by diagenesis (e.g. San Miguel et al., 2017b). Previous studies on upper Kimmeridgian mid-ramp successions in NE Spain (San Miguel et al.,

2017c) have documented diagenetic processes prior to compaction affecting grainstone and reefal sedimentary bodies. Such processes include cementation, pore-enhancing processes such as the micritization of carbonate grains, and reflux dolomitization. Dolomitization is also observed in the Higueruelas Fm, particularly in northern areas (i.e. the localities of Muel and Jaulín; see Fig. 2), and has been tentatively related to hydrothermal fluids circulating through normal faults reactivated during the Alpine compression (Aurell, 1990). Hydrothermal dolomitization has also been proposed for age-equivalent carbonate rocks of the neighbouring Maestrat Basin (e.g. Rodríguez-Morillas et al., 2013; Travé et al., 2019). The sedimentological heterogeneities (i.e. dimension and lateral extent) revealed for the potential reservoir facies in the studied successions of the Higueruelas Fm make these shallow-marine deposits the target of future studies focusing on their diagenetic heterogeneities.

6.3. Comparison with other similar environments

The distribution of the Kimmeridgian carbonate facies from shallow to relatively deep offshore settings has previously been documented in the successions deposited in southern marginal areas of the Iberian Basin. In the shallow-platform facies of the sequence Ki2 (Torrecilla Fm; Fig. 1C), Bádenas and Aurell (2010) described sand-shoal deposits dominated by variable proportions of peloids and type 3 and 1/3 ooids, with variations in their lateral extent comparable to those observed in the Higueruelas Fm (i.e. 3-12 km, see Figs 13 and 14). Oncolitic-dominated facies are also recorded in this environment: type I and II oncoid G facies replaced the oolitic shoals in specific areas of the ramp; *Bacinella*-oncoids were widespread in a low-energy lagoon; and type III oncoids were generally deposited offshore, laterally related to coral reefs. In contrast, for the latest Kimmeridgian carbonate ramp studied in this work, specific hydrodynamic conditions partly controlled by the irregular bottom topography led to a wider distribution of oncoids partly or completely dominated by organism-bearing encrustations (i.e. type II, III and IV oncoids), being abundant in the sheltered lagoon and areas of the backshoal, shoal-sand blanket and foreshoal subenvironments.

As regards shallow carbonate environments in Kimmeridgian successions outside the Iberian Basin, of particular interest for hydrocarbon exploration are the upper Kimmeridgian carbonate ramp deposits of the Arab-D Fm (Ayoub and En Nadi, 2000; Al-Saad and Ibrahim, 2005). Significant facies in the Arab-D reservoirs are the well-sorted oolitic packstone-grainstone facies forming active shoals, and stromatoporoid-dominated buildups in the foreshoal environment. This set of facies shows a significant difference regarding the dimension of the stromatoporoid-rich facies, as large-scale stromatoporoid reefs arranged as belts occur in the Arab-D deposits, instead of the patchy distribution of the stromatoporoid buildups in the studied Higueruelas Fm. Lagoonal stromatoporoid carpets have been recorded in the Higueruelas Fm, but also in sequence Ki2 (Jabaloyas outcrop; San Miguel et al., 2017a), a stromatoporoid facies not recorded in the Arab-D Fm. Lehmann et al. (2010) recognized m-thick stromatoporoid buildups from middle to outer-ramp areas of the Upper Jurassic carbonate platform in offshore Abu Dhabi (eastern Saudi Arabia), more than 3 km in lateral extent. In contrast, the chaetetid-stromatoporoid-coral buildups characterized in the Higueruelas Fm are recognized in relatively proximal areas of the middle ramp, and are no more than 250 m in lateral extent.

The overall lateral extent of the sand-shoal complex in the Upper Jurassic Arab Fm reaches 17 to 20 km in width, whereas in the carbonate ramp under study the lateral extent of the shoal-sand blankets ranges from 3 to 12 km. Previous studies of similar carbonate shoals in the Upper Muschelkalk (Middle Triassic) have documented a high degree of lateral continuity of high-energy shoal lithofacies at scales from a few km to > 10 km in dip- and strike directions (e.g. Ruf and Aigner, 2004; Petrovic and Aigner, 2017). In relation to the particular lateral migration of the shoal-sand blanket described in this work, Marchionda et al. (2018) also document different directions of progradation of oolitic shoals in the Kimmeridgian-Tithonian shallow carbonate ramp of the Arab Fm (onshore Abu Dhabi), suggesting a local topographic control related to halokinetic activity in the substratum (i.e. substratum diapiric motions leading to local changes in accommodation). This situation diverges from the sedimentary control on the lateral migration of the shoal-sand blanket sediment described in the present paper, which has been related primarily to the redistribution of the sediment by hydrodynamic factors.

7. Conclusions

The complexity of the spatial facies distribution and sedimentary evolution of the inner- to mid-ramp areas of a latest Kimmeridgian shallow carbonate ramp (Higueruelas Fm, north-central Iberian Basin) has been deciphered, highlighting the combined role of the external and internal factors operating on these shallow marine environments. The overall facies evolution reflects a long-term shallowing-upward trend, related to the long-term fall in sea level that occurred during the late Kimmeridgian in the Iberian Basin.

Analysis of the vertical and lateral facies distribution in nine sedimentary units has allowed us to propose two sedimentary models of ramp evolution, with significant variations in facies belts and the presence of facies mosaics in specific areas of the ramps. The oncolitic-peloidal-oolitic-dominated carbonate ramp (sedimentary units 1-4) included an intertidal belt characterized by peloidal mudstones to packstone-grainstones with fenestral porosity, a low-energy sheltered lagoon characterized by an abundance of large type IV oncoids, and oolitic-peloidal backshoal, shoal-sand blanket and foreshoal subenvironments, which grade offshore to bioclastic-peloidal mudstones. Oncolitic-dominated packstones to grainstones developed along strike in high-energy areas, and a mosaic of stromatoporoid carpets and chaetetid-stromatoporoid-coral buildups also accumulated in inner- to mid-ramp domains, respectively.

A significant shift in the palaeoenvironmental conditions, probably related to higher-energy conditions and increased terrigenous supply, took place during the deposition of sedimentary units 5 to 9, giving rise to an oolitic-peloidal-dominated carbonate ramp, with very local records of oncolitic facies. This ramp included a wide restricted lagoon, without stromatoporoid-rich carpets, and peloidal-dominated backshoal, shoal-sand blanket and foreshoal subenvironments, with frequent intraclastic-peloidal storm-related deposits. Chaetetid-stromatoporoid-coral buildups developed offshore, in the mid-ramp setting.

Variations in hydrodynamic factors (waves and storms) and sea-bottom topography controlled the observed along-strike and down-dip variations in lateral extent and in the predominant non-skeletal content that developed especially in inner-ramp areas. Backshoal, shoal-sand blanket and foreshoal grain-supported facies, with lithic peloids and ooids, developed in higher-energy areas, whereas oncoids were

concentrated in depressed areas of the shoal body. Inshore in the lagoon, low-energy conditions favoured bacterial growth in oncoids and the development of stromatoporoid-rich carpets, whereas fluctuations in salinity, energy and siliciclastic input resulted in a peloidal-bioclastic-oolitic lagoon without oncoids or stromatoporoids. The influence of probable short eccentricity cycles is inferred from the time span of the studied sequence Ki3 and the lateral continuity of the bounding surfaces of the nine identified sedimentary units (i.e. high-frequency sequences) within Ki3. Eccentricity-related sea-level fluctuations, internal processes of sediment production and redistribution, and long-term regression controlled the variable sedimentary trends observed within these high-frequency sequences.

The facies distribution and down-dip heterogeneities summarized in the two proposed carbonate-ramp models can be applied to the interpretation of shallow carbonate platforms that include similar non-skeletal components. In particular, the reported data lead to a detailed description of the distribution and lateral extent of oolitic, peloidal, oncolitic and stromatoporoid-rich grain-supported facies, which can be useful in reservoir characterization.

Acknowledgments

This paper was funded by projects CGL2017-85038-P and Group E18 (Aragosaurus: Recursos Geológicos y Paleoambientales) subsidized by the Spanish Ministry of Science and Innovation, the European Regional Development Fund and the Government of Aragón. The research of Cristina Sequero is funded by a FPU Grant (Spanish Ministry of Science and Innovation). The authors would like to acknowledge the financial support from the International Association of Sedimentologists (IAS Postgraduate Grant Scheme) and the use of the Servicio General de Apoyo a la Investigación-SAI, Universidad de Zaragoza. We also thank Laura Tomassetti and André Strasser for the revision, and Rupert Glasgow for accepting to review the English quality.

References

Al-Awwad, S.F., Collins, L.B., 2013. Arabian carbonate reservoirs: A depositional model of the Arab-D reservoir in Khurais field, Saudi Arabia. AAPG 97, 1099-1119.

Al-Saad, H., Ibrahim, M., 2005. Facies and palynofacies characteristics of the Upper Jurassic Arab D reservoir in Qatar. Revue de Paléobiologie 24 (1), 225-241.

Amour, F., Mutti, M., Christ, N., Inmenhauser, A., Benson, G.S., Agar, S.M., Tomás, S., Kabiri, L., 2013. Outcrop analog for an oolitic carbonate reservoir: A scale-dependent geologic modeling approach based on stratigraphic hierarchy. AAPG 97 (5), 845-871.

Aurell, M., 1990. El Jurásico Superior en la Cordillera Ibérica Central (provincias de Zaragoza y Teruel). Análisis de cuenca. PhD Thesis, Zaragoza University.

Aurell, M., Meléndez, A., 1986. Sedimentología de la Formación Calizas con oncolitos de Higueruelas (Malm) en la región de Muel-Belchite (Provincia de Zaragoza). Acta Geológica Hispánica 21-22, 307-312.

Aurell, M., Meléndez, A., 1987. Las bioconstrucciones de corales y sus facies asociadas durante el Malm en la Cordillera Ibérica Central (prov. de Zaragoza). Estudios Geológicos 43, 261-269.

Aurell, M., Robles, S., Bádenas, B., Rosales, I., Quesada, S., Meléndez, G., García-Ramos, J.C., 2003. Transgressive-regressive cycles and Jurassic palaeogeography of northeast Iberia. Sediment. Geol. 162, 239-271.

Aurell, M., Bádenas, B., Ipas, J., Ramajo, J., 2010. Sedimentary evolution of an Upper Jurassic epeiric carbonate ramp, Iberian Basin, NE Spain. In: Van Buchem, F.S.P., Gerdes, K.D., Esteban, M. (Eds.), Mesozoic and Cenozoic Carbonate Systems of the Mediterranean and the Middle East: Stratigraphic and Diagenetic Reference Models. Geol. Soc. London Spec. Public. 329, pp. 89-111.

Aurell, M., Ipas, J., Bádenas, B., Muñoz, A., 2012. Distribución de facies con corales y estromatopóridos en el dominio interno de una plataforma carbonatada (Titónico, Cordillera Ibérica). Geogaceta 51, 67-70.

Aurell, M., Bádenas, B., Canudo, J.I., Castanera, D., García-Penas, A., Gasca, J.M., Martín-Closas, C., Moliner, L., Moreno-Azanza, M., Rosales, I., Santás, L., Sequero, C., Val, J. Kimmeridgian-Berriasian stratigraphy and sedimentary evolution of the central Iberian Rift System (NE Spain). Cretaceous Research (in press).

Ayoub, R., En Nadi, I.M., 2000. Stratigraphic framework and reservoir development of the Upper Jurassic in Abu Dhabi area, U.A.E. In: Alsharhan, A.S., Scott, R.W. (Eds.), Middle East Models of Jurassic/Cretaceous Carbonate System 69, pp. 229-248.

Bacelle, L., Bosellini, A., 1965. Diagrammi per la stima visiva della composizione percentuale nelle rocce sedimentarie. Ann. Uni. Ferrara, N.S., Sez. IX: Sci. Geol. Paleontol 1, 59-62.

Bádenas, B., Aurell, M., 2001. Kimmeridgian palaeogeography and basin evolution of northeastern Iberia. Palaeogeogr., Palaeoclimatol., Palaeoeco. 168, 291-310.

Bádenas, B., Aurell, M., 2003. Análisis comparado y controles en la sedimentación de dos arrecifes de la zona media de una rampa carbonatada del Jurásico Superior de la Cordillera Ibérica. Rev. Soc. Geol. España 16 (3-4), 151-166.

Bádenas, B., Aurell, M., 2010. Facies models of a shallow-water carbonate ramp based on distribution of non-skeletal grains (Kimmeridgian, Spain). Facies 56, 89-110.

Bádenas, B., Aurell, M., 2018. The Down-dip Preferential Sequence Record of Orbital Cycles in Greenhouse Carbonate Ramps: Examples From the Jurassic of the Iberian Basin (NE Spain). In: Montenari, M. (Ed.), Stratigraphy and Timescales 3, pp. 285-325.

Bádenas, B., Aurell, M., Rodríguez-Tovar, F.J., Pardo-Igúzquiza, E., 2003. Sequence stratigraphy and bedding rhythms of an outer ramp limestone succession (Late Kimmeridgian, Northeast Spain). Sediment. Geol. 161, 153-174.

Bádenas, B., Salas, R., Aurell, M., 2004. Three orders of regional sealevel changes control facies and stacking patterns of shallow platform carbonates in the Maestrat Basin (Tithonian-Berriasian, NE Spain). Int. J. Earth Sci. (Geol Rundsch) 93, 144-162.

Bádenas, B., Aurell, M., Gröcke, D.R., 2005. Facies analysis and correlation of high-order sequences in middle-outer ramp successions: variations in exported carbonate in basinwide d13C (Kimmeridgian, NE Spain). Sedimentology 52, 1253–1276.

Bádenas, B., Aurell, M., Bosence, D., 2010. Continuity and facies heterogeneities of shallow carbonate ramp cycles (Sinemurian, Lower Jurassic, North-east Spain). Sedimentology 57, 1021-1048.

Borkhataria, R., Aigner, T., Pöppelreiter, M.C., Pipping, J.C.P., 2005. Characterization of epeiric "layer-cake" carbonate reservoirs: Upper Muschelkalk (Middle Triassic), The Netherlands. J. Petroleum Geol. 28, 119-146.

Burchette, T.P., Wright, V.P., 1992. Carbonate ramp depositional systems. Sediment. Geol. 79, 3-57.

Cortés Gracia, A.L., Casas Sainz, A.M., 1996. Deformación alpina de zócalo y cobertera en el borde norte de la Cordillera Ibérica (Cubeta de Azuara-Sierra de Herrera). Rev. Soc. Geol. España 9 (1-2), 51-66.

Dahanayake, K., 1977. Classification of oncoids from the Upper Jurassic carbonates of the French Jura. Sediment. Geol. 18, 337-353.

Dahanayake, K., 1978. Sequential position and environmental significance of different types of oncoids. Sediment. Geol. 20, 301-316.

Della Porta, G., Kenter, J.A.M., Immenhauser, A., Bahamonde, J., 2002. Lithofacies character and architecture across a Pennsylvanian inner-platform transect (Sierra de Cuera, Asturias, Spain). J. Sed. Res. 72, 898-916.

Dercourt, J., Ricou, L., Vrielynck, B., 1993. Atlas: Tethys palaeoenvironmental Maps. CCGM, Paris.

Droste, H., 2006. A new model for epeiric carbonate platforms. GEO 2006 Middle East Conference and Exhibition 27-29 March 2006. Manama, Bahrain.

Dunham, R.J., 1962. Classification of carbonate rocks according to depositional texture. AAPG Memoir 1, 108-121.

Dupraz, C., Strasser, A., 1999. Microbialites and micro-encrusters in shallow coral bioherms (Middle to Late Oxfordian, Swiss Jura mountains). Facies 40, 101-129.

Flügel, E., 1974. Fazies-Interpretation der *Cladocoropsis*-Kalke (Malm) auf Karaburun, W-Anatolien. Arch Lagerstätt-Forsch Ostalpen Sd-Bd 2, 79-94.

Flügel, E., 2004. Microfacies of Carbonate Rocks. Analysis, Interpretation and Application. Springer-Verlag, Germany.

Golonka, J., Ross, M.J., Scotese, C.R., 1994. Phanerozoic paleogeographic and paleoclimatic modeling maps. In: Pangea: Global Environments and Resources. Canadian Society of Petroleum Geologists, Memoir 17, pp. 1-47.

Grötsch, J., Suwaina, O., Ajlani, G., Taher, A., El-Khassawneh, R., Lokier, S., Coy, G., van der Weerd, E., Masalmeh, S., van Dorp, J., 2003. The Arab Formation in central Abu Dhabi: 3-D reservoir architecture and static and dynamic modelling. GeoArabia, Gulf PetroLink, Bahrain 8 (1), 47-86.

Harris, P.M., Purkis, S.J., Ellis, J., Swart, P.K., Reijmer, J.J.G., 2014. Mapping bathymetry and depositional facies on Great Bahama Bank. Sedimentology 62, 566-589.

Hillgärtner, H., 2006. High-resolution correlation in Cretaceous platform carbonates of the Middle East: rules to solve the puzzle?. AAPG European Region Conference: Architecture of Carbonate Systems Through Time, Mallorca 2006, Program Book 26.

Hönig, M.R., John, C.M., 2015. Sedimentological and isotopic heterogeneities within a Jurassic carbonate ramp (UAE) and implications for reservoirs in the Middle East. Mar. Pet. Geol. 68, 240-257.

Hughes, G.W., 2004. Middle to Upper Jurassic Saudi Arabian carbonate petroleum reservoirs: biostratigraphy, micropaleontology, and paleoenvironments. GeoArabia 9, 79-114.

Ipas, J., Aurell, M., Bádenas, B., 2004. Ambientes sedimentarios y secuencias en la Fm. Higueruelas (Jurásico Superior) en la Cordillera Ibérica Septentrional. Geogaceta 35, 7-10.

Ipas, J., Aurell, M., Bádenas, B., Canudo, J.I., Liesa, C., Mas, J.R., Soria, A.R., 2007. Caracterización de la Formación Villar del Arzobispo al sur de Zaragoza (Titónico, Cordillera Ibérica). Geogaceta 41, 111-114.

Kerans, C., Tinker, S.W., 1997. Sequence stratigraphy and Characterization of Carbonate Reservoirs. SEMP Short Courses Notes 40. SEMP, Tulsa, OK.

Lehmann, C.T., Al Hosany, K.I., Matarid, T., Sayed, M.I., 2010. Addressing Reservoir Heterogeneities in the Development of Upper Jurassic Carbonate Reservoirs, offshore Abu Dhabi. Society of Petroleum Engineers, SPE 137888.

Leinfelder, R.R., Nose, M., Schmid, D., Werner, M., 1993. Microbial Crusts of the Late Jurassic: Composition, Palaeoecological Significance and Importance in Reef Construction. Facies 29, 195-230.

Leinfelder, R.R., Schlagintweit, F., Werner, W., Ebli, O., Nose, M., Schmid, D., Hughes, G., 2005. Significance of stromatoporoids in Jurassic reefs and carbonate platforms-concepts and implications. Facies 51, 287-325.

Lindsay, R.F., Cantrell, D.L., Hughes, G.W., Keith, T.H., Mueller H.W. III, Russel, D., 2006. Ghawar Arab-D reservoir: widespread porosity in shoaling-upward carbonate cycles. Saudi Arabia AAPG Mem. 88, 97-138.

Marchionda, E., Deschamps, R., Gobianchi, M., Nader, F.H., Di Giulio, A., Morad, D.J., Al Darmaki, F., Ceriani, A., 2018. Field-scale depositional evolution of the Upper Jurassic Arab Formation (onshore Abu Dhabi, UAE). Mar. Pet. Geol. 89, 350-369.

Marsaglia, K.M., Klein, G.deV., 1983. The palaeogeography of Paleozoic and Mesozoic storm depositional systems. J. Geol. 91, 117-142.

Petrovic, A., Aigner, T., 2017. Are shoal reservoirs discrete bodies? A coquina shoal outcrop analogue from the Mid-Triassic Upper Muschelkalk, SW Germany. J. Pet. Geol. 40 (3), 249-275.

Pomar, L., 2018. Carbonate factories through the Earth History. EGU General Assembly Conference Abstracts 20, 3861.

Pomar, L., Kendall, C.S.C., 2007. Architecture of carbonate platforms: a response to hydrodynamics and evolving ecology. In: Lukasik, J., Simo, J.A. (Eds.), Controls on Carbonate Platform and Reef Development, vol. 89. SEPM Spec. Publ., Tulsa, OK, pp. 187-216.

Pomar, L., Aurell, M., Bádenas, B., Morsilli, M., Al-Awwad, S.F., 2015. Depositional model for a prograding oolitic wedge, Upper Jurassic, Iberian Basin. Mar. Pet. Geol. 67, 556-582.

Price, G.D., Sellwood, B.W., Valdes, P.J., 1995. Sedimentological evaluation of general circulation model simulations for the “greenhouse” Earth: Cretaceous and Jurassic case studies. Sediment. Geol. 100, 159-180.

Purkis, S., Casini, G., Hunt, D., Colpaert, A., 2015. Morphometric patterns in modern carbonate platforms can be applied to the ancient rock record: similarities between modern Alacranes Reef and Upper Palaeozoic platforms of the Barents Sea. Sediment. Geol. 321, 49-69.

Rankey, E.C., Reeder, S.L., 2011. Holocene oolitic Marine sand complexes of the Bahamas. J. Sediment. Res. 81, 97-117.

Reijmer, J.J.G., Swart, P.K., Bauch, T., Otto, R., Reuning, L., Roth, S., Zechel, S., 2009. A re evaluation of facies on Great Bahama Bank I: New facies maps of western Great Bahamas Bank. In: Swart, P.K., Eberli, G.P., McKenzie, J.A. (Eds.), Perspectives in Carbonate Geology. IAS Spec. Publ. 41, pp. 29-46.

Riding, R., 2002. Structure and composition of organic reefs and carbonate mud mounds: concepts and categories. Earth Sci. Rev. 58, 163-231.

Riegl, B., Piller, W.E., 2000. Reefs and coral carpets in the Miocene paratethys (Badenian, Leitha Limestone, Austria). Mar. & Env. Sci. Faculty Proceedings, Presentations, Spechees, Lectures 111.

Rodríguez-Morillas, N., Playà, E., Travé, A., Martín-Martín, J.D., 2013. Diagenetic processes in a partially dolomitized carbonate reservoir: Casablanca oil field, Mediterranean Sea, offshore Spain. Geol. Acta 11(2), 195-214.

Ruf, M., Aigner, T., 2004. Facies and poroperm characteristics of a carbonate shoal (Muschelkalk, South German Basin): A reservoir analogue investigation. J. Pet. Geol. 27, 215-239.

Salas, R., Casas, A., 1993. Mesozoic extensional tectonics, stratigraphy and crustal evolution during the Alpine cycle of the eastern Iberian basin. Tectonophysics 228, 33-55.

Salas, R., Guimerà, J., Mas, R., Martín-Closas, C., Meléndez, A., Alonso, A., 2001. Evolution of the Mesozoic central Iberian Rift System and its Cainozoic inversion (Iberian chain). In: Ziegler, P.A., Cavazza, W., Robertson, A.H.F., Crasquin-Soleau, S. (Eds.), Peri-Tethys Memoir 6: Peri-Tethyan Rift/Wrench and Passive Margins. Mém. Mus. Natn. Hist. nat. 186, pp. 145-185.

San Miguel, G., Aurell, M., Bádenas, B., 2017a. Occurrence of high-diversity metazoan- to microbial-dominated bioconstructions in a shallow Kimmeridgian carbonate ramp (Jabaloyas, Spain). Facies 63, 13.

San Miguel, G., Aurell, M., Bádenas, B., 2017b. Diagenetic evolution of a shallow marine Kimmeridgian carbonate ramp (Jabaloyas, NE Spain): implications for hydrocarbon reservoir quality. Arab. J. Geosci. 10, 376.

San Miguel, G., Duaso, M., Prados, G., Aurell, M., Kenter, J., 2017c. Early diagenetic events in Late Kimmeridgian carbonate ramps (Iberian Basin, NE Spain): implications for outcrop characterization and deciphering and prediction of carbonate reservoir heterogeneitiy. 33rd International Meeting of Sedimentology, pp. 803.

Sequero, C., Bádenas, B., Aurell, M., 2018. Facies mosaic in the inner areas of a shallow carbonate ramp (Upper Jurassic, Higueruelas Fm, NE Spain). Facies 64, 9.

Shinn, E.A., 1968. Practical significance of birdseye structures in carbonate rocks. Jour. Sed. Petrology 38, 215-223.

Strasser, A., 1986. Ooids in Purbeck limestones (Lowermost Cretaceous) of the Swiss and French Jura. Sedimentology 33, 711-727.

Strasser, A., 2018. Cyclostratigraphy of Shallow-Marine Carbonates-Limitations and Opportunities. In: Montenari, M. (Ed.), Stratigraphy and Timescales 3, pp. 151-187.

Strasser, A., Védrine, S., 2009. Controls on facies mosaics of carbonate platforms: a case study from the Oxfordian of the Swiss Jura. In: Swart, P., Eberli, G., McKenzie, J. (Eds.), Perspectives in Carbonate Geology: a Tribute to the Career of Robert Nathan Ginsburg, vol. 41 IAS Spec. Publ., pp. 199-213.

Strasser, A., Pittet, B., Hillgärtner, H., Pasquier, J.B., 1999. Depositional sequences in shallow carbonate-dominated sedimentary systems: concepts for a high-resolution analysis. Sed. Geol. 128, 201-221.

Tomás, S., Zitzmann, M., Homman, M., Rumpf, M., Amour, F., Benisek, M., Marcano, G., Mutti, M., Betzler, C., 2010. From ramp to platform: building a 3D model of depositional geometries and facies architectures in transitional carbonates in the Miocene, northern Sardinia. Facies 56, 195-210.

Tomassetti, L., Petracchini, L., Brandano, M., Trippetta, F., Tomassi, A., 2018. Modeling lateral facies heterogeneity of an upper Oligocene carbonate ramp (Salento, southern Italy). Mar. Pet. Geol. 96, 254-270.

Travé, A., Nadal, J., Playà, E., Salas, R., Martín-Martín, J.D., Gomez-Rivas, E., 2019. Fracture-related dolomitization affecting Late Jurassic-Lowermost Cretaceous syn-rift deposits (Maestrat Basin, southern Iberian Chain, Eastern Spain). In: Doronzo, D.M., et al. (Eds.), Petrogenesis and Exploration of the Earth's Interior, pp. 163-165.

Turnsek, D., Buser, S., Ogorelec, B., 1981. An Upper Jurassic reef complex from Slovenia, Yugoslavia. In: Toomey, D.F. (Ed), European fossil reef models. SEPM Spec. Publ. 30, 361-369.

Wender, L.E., Bryant, J.W., Dickens, M.F., Neville, A.S., Al-Moqbel, A.M., 1998. Paleozoic (pre-Khuff) hydrocarbon geology of the Ghawar area, eastern Saudi Arabia. GeoArabia 3, 273-301.

Wilkinson, B.H., Drummond, C.N., Diedrich, N.W., Rothman, E.D., 1999. Poisson processes of carbonate accumulation on Paleozoic and Holocene platforms. J. Sediment. Res. 69, 338-350.

Figure captions

Figure 1. (A) Palaeogeography of western Europe during the late Kimmeridgian (modified from Dercourt et al., 1993). (B) Main facies belts in the northeastern Iberian Basin during the late Kimmeridgian (compiled from Aurell et al., 2003 and Ipas et al., 2004). (C) Synthetic stratigraphy of the Kimmeridgian in the northern Iberian Basin including the main facies belts (modified from Aurell et al., 2010, in press). The Higueruelas Fm corresponds to the sequence Ki3. (D) Field view of the Higueruelas Fm, the underlying Loriguilla Fm and the overlying coastal siliciclastic-dominated deposits. The lower and upper boundaries of the Higueruelas Fm correspond to basin-wide discontinuity surfaces.

Figure 2. Extent of the Jurassic outcrops and location of the studied logs south of Zaragoza (northeast Spain) (modified from Cortés and Casas, 1996). Dashed lines indicate the cross-sections shown in Figs 5-7.

Figure 3. Correlation between the studied logs in the three cross-sections, based on the identification of time-equivalent sharp bedding surfaces (black lines), which allowed nine sedimentary units (1-9) to be documented. This best-fit solution is coherent with the vertical facies trends observed within the sedimentary units. The lower and upper datum for correlation is also indicated (red and blue lines, respectively), as well as the eroded areas in the upper part, prior to the deposition of Cenozoic sediments.

Figure 4. Vertical facies evolution within the sedimentary units (1-7) identified for the Higueruelas Fm in the stratigraphic sections A1 and TO (see Fig. 2 for location). White lines indicate the position of the sharp bedding planes.

Figure 5. Facies distribution in the northern cross-section.

Figure 6. Facies distribution in the central cross-section.

Figure 7. Facies distribution in the southern cross-section.

Figure 8. (a) Fenestral porosity (intertidal subenvironment) in peloidal mudstone facies. (b, c) Restricted lagoon facies with well-sorted lithic peloids, bioclasts (bivalves, lituolids: b and dashed arrow in c, respectively) and type 3 ooids (white arrow in c), showing thinly laminated fine-radial cortices. (d-f) Backshoal facies with poorly sorted peloids, type II oncoids (white arrow in d), protected-marine bioclasts (dasycladacean algae: black arrow in e), type 1/3 ooids and aggregate grains (white and dashed arrows in f, respectively). (g) Backshoal peloidal facies with intense burrowing. (h) Storm-related deposit with mm- to cm-sized intraclasts and poorly sorted peloids. Facies symbols are included in the pictures (see facies legend in Figs 5 to 7).

Figure 9. (a-c) Peloidal to oolitic shoal-sand blanket facies composed of well-sorted lithic peloids, type 1 and 1/3 ooids and scarce bioclasts. (d) Well-sorted lithic peloids in foreshoal facies with some bioclasts (e.g. lituolids: white arrow). (e) Offshore-proximal facies with lituolids (white arrow) and poorly sorted peloids. (f) Sponge spicules in bioclastic-peloidal mudstone facies (offshore-distal subenvironment).

Figure 10. (a) Well-sorted peloids, micritized bioclasts, ooids and type I oncoids in gastropod-oncolitic facies, with mainly gastropods as bioclastic cores (white arrow). (b, c) Oncolitic facies in sheltered lagoon subenvironment in macro-scale example (b) and thin section (c), with type IV oncoids composed of a microbial meshwork (white arrow in c). (d, e) Macro-scale examples of type III oncoid-dominated facies with oncolitic-supported texture. (f) Type III oncoid (white arrow) in backshoal oncolitic-dominated facies, composed of alternating micritic and organism-bearing laminae of similar thickness. (g) Type II oncoids in shoal-sand blanket oncolitic-dominated facies, composed of thick micritic laminae with organism-bearing encrustations.

Figure 11. (a-d) Stromatoporoid-rich facies in sheltered lagoon subenvironment. (a, b) Fragments of *Cladocoropsis*, poorly sorted peloids, microbial peloids and micritized bioclasts in stromatoporoid W to G facies. Stromatoporoids appear as isolated cm-sized fragments (black arrow in b) surrounding by a matrix composed of peloids, ooids and bioclasts (dashed arrow in b). *Tubiphytes* encrustations are common on stromatoporoids (white arrow in b). (c) Microbial peloids (white arrows) and *Tubiphytes* (black arrow) in stromatoporoid-rich facies. (d) Type II oncoid with bioclastic core (coral; white arrow) and thin crust with micritic laminae and organism-bearing encrustations in oncolitic-stromatoporoid W to G facies. (e-h) Chaetetid-stromatoporoid-coral buildup (e, f) and inter-buildup stromatoporoid-chaetetid-coral and oncolitic W to G (g, h) facies, showing fragments of chaetetids, microbial crusts with internal cavities (white and dashed arrows in e, respectively), and type II oncoids in inter-buildup facies (dashed arrow in g). (f) Macro-scale example of microbial crusts (white arrow) in chaetetid-stromatoporoid-coral

buildup facies. (h) Macro-scale example of inter-buildup stromatoporoid-chaetetid-coral and oncolitic W to G facies, showing fragments of chaetetids (white arrow), bioclasts and oncoids (dashed arrows).

Figure 12. Field view and facies distribution of chaetetid-stromatoporoid-coral buildup, inter-buildup stromatoporoid-chaetetid-coral and oncolitic W to G, and offshore-proximal peloidal-bioclastic W to P facies in unit 4 of the stratigraphic section F5 (see Fig. 2 for location) (modified from Bádenas and Aurell, 2003).

Figure 13. Facies maps reconstructed for sedimentary units 1 to 4**.**

Figure 14. Facies maps reconstructed for sedimentary units 5 to 9.

Figure 15. Sedimentary models showing the facies distribution of the latest Kimmeridgian carbonate ramp during the deposition of sedimentary units 1-4 (A) and 5-9 (B).

Figure 16. Summary of the facies and non-skeletal component distribution for the two proposed sedimentary models. Black and grey horizontal bars indicate the abundance of non-skeletal grains (type I-II oncoid distribution in the oncolitic-peloidal-oolitic-dominated ramp refers mainly to type II oncoids, as type I oncoids generally appear in low abundance). The distribution of stromatoporoid/chaetetid/coral-rich facies is also included.

Figure 17. Sedimentary trends within the high-frequency sequences (1 to 8) recognized in the MU-J2-J3-V transect, based on lateral facies relationships observed in the reconstructed palaeogeographic maps (see Figs 13 and 14). Characteristics of the sequence boundaries are also included. Notice the variability of the vertical sedimentary trend of a single correlated high-frequency sequence between closely-spaced sections.

Figure 18. Lateral and vertical distribution of the grain-supported facies (packstone-grainstone and grainstone textures) in the studied cross-sections. The distribution of stromatoporoid-rich carpets and buildups is also included.

Table 1. Characteristics of the main non-skeletal grains.

Table 2. Facies description.

Table 3. Skeletal components in Table 2.

Figure

Click here to download high resolution image

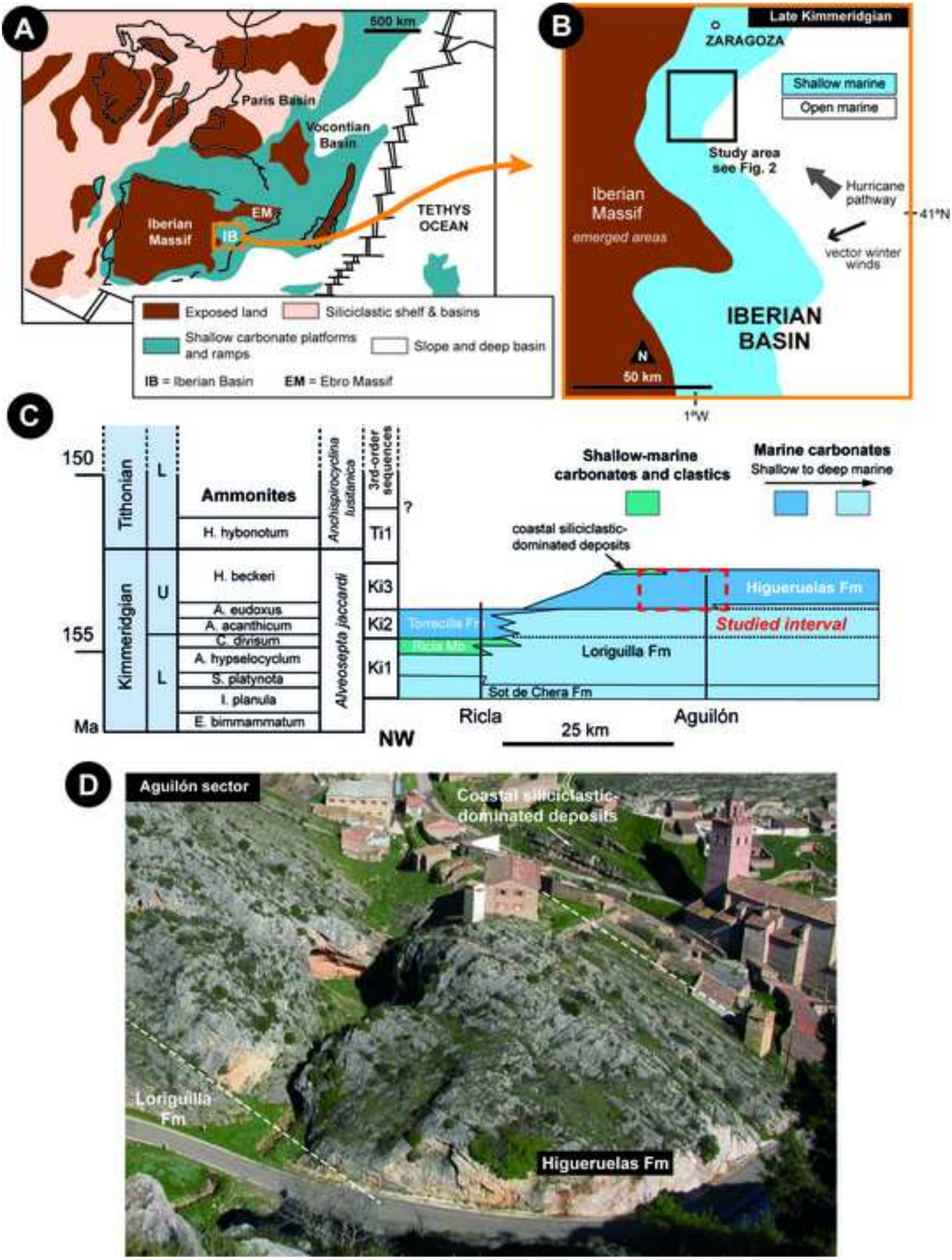

Figure 2

Click here to download high resolution image

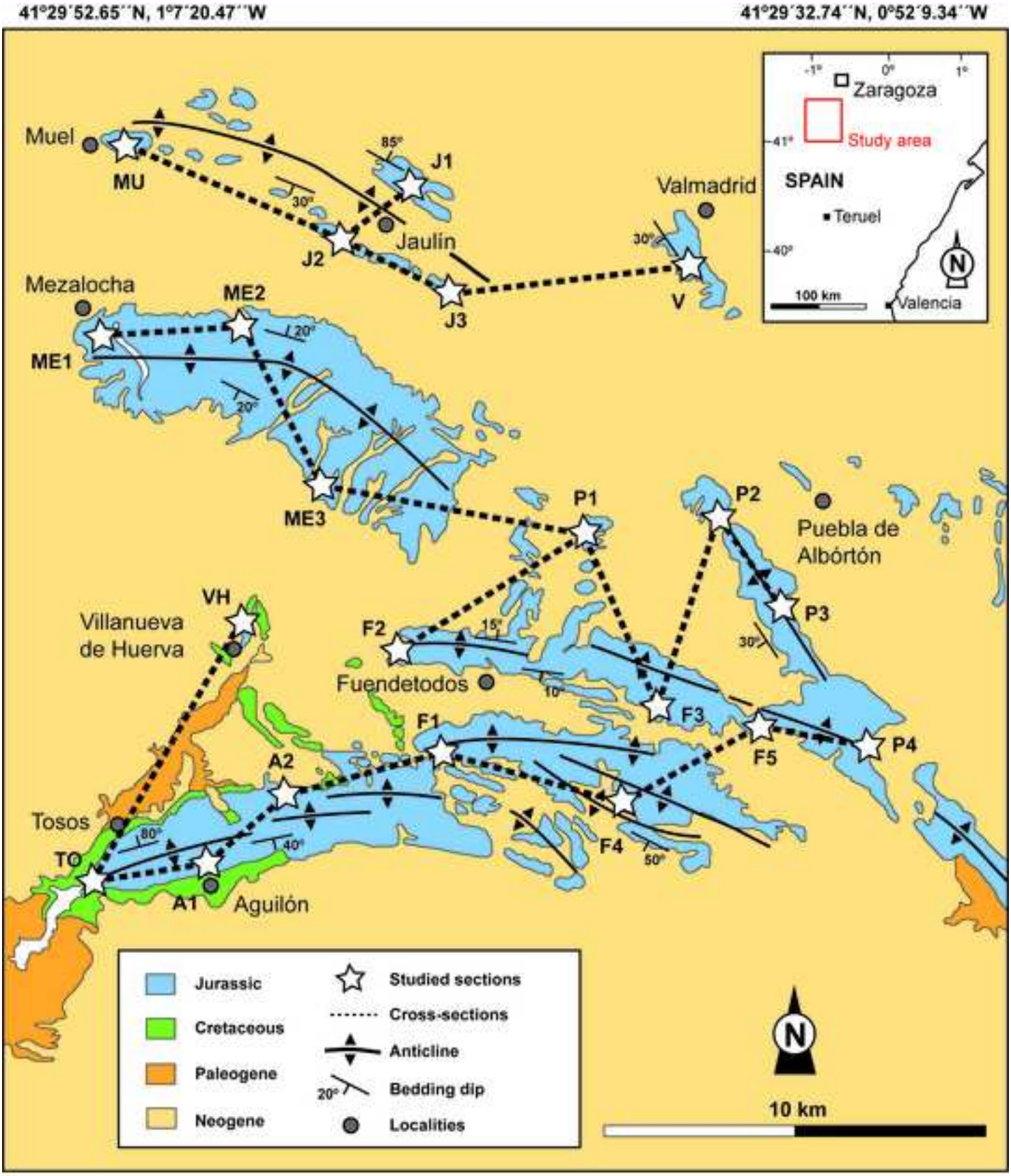

Figure 3

Click here to download high resolution image

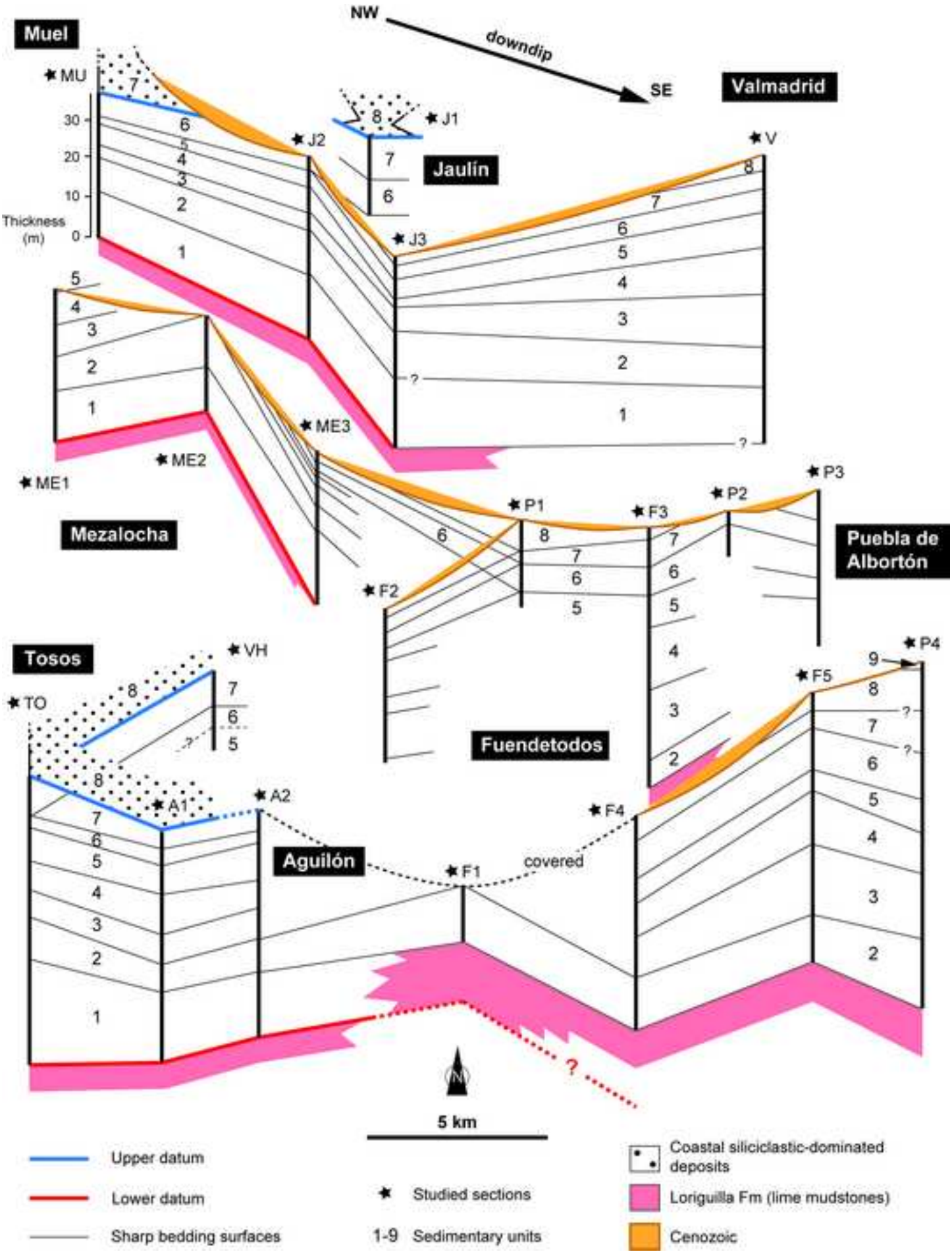

Figure 4

Click here to download high resolution image

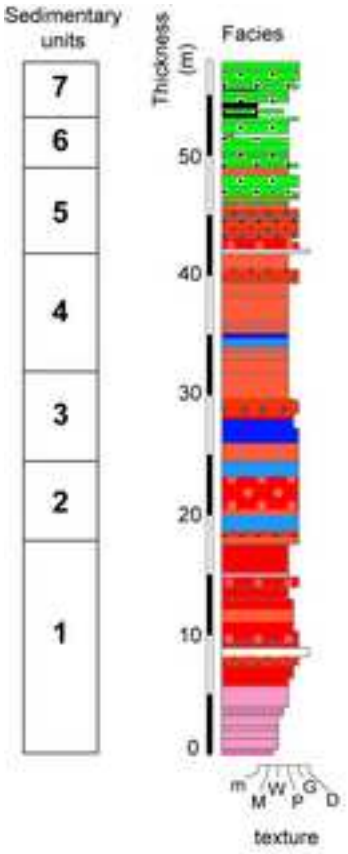

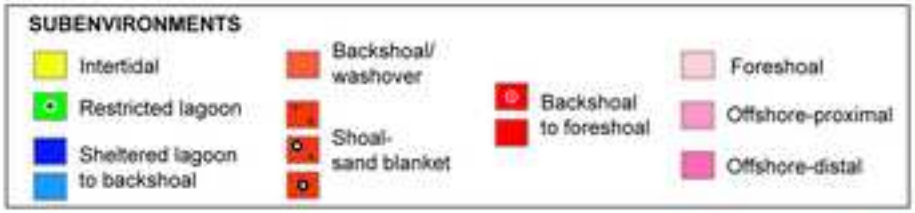

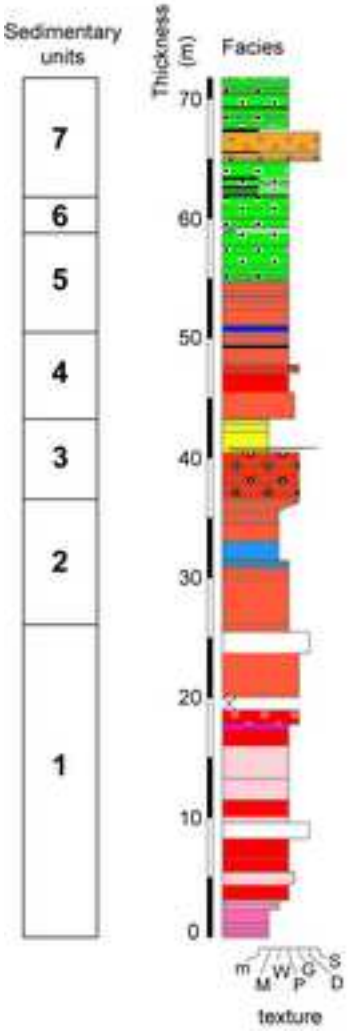

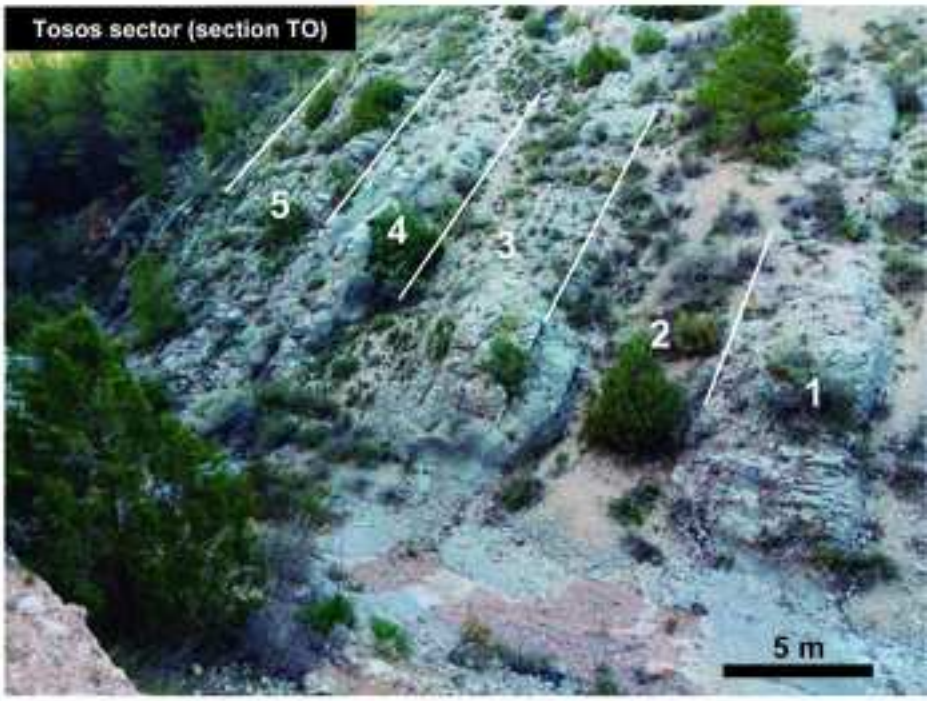

Figure 5

Click here to download high resolution image

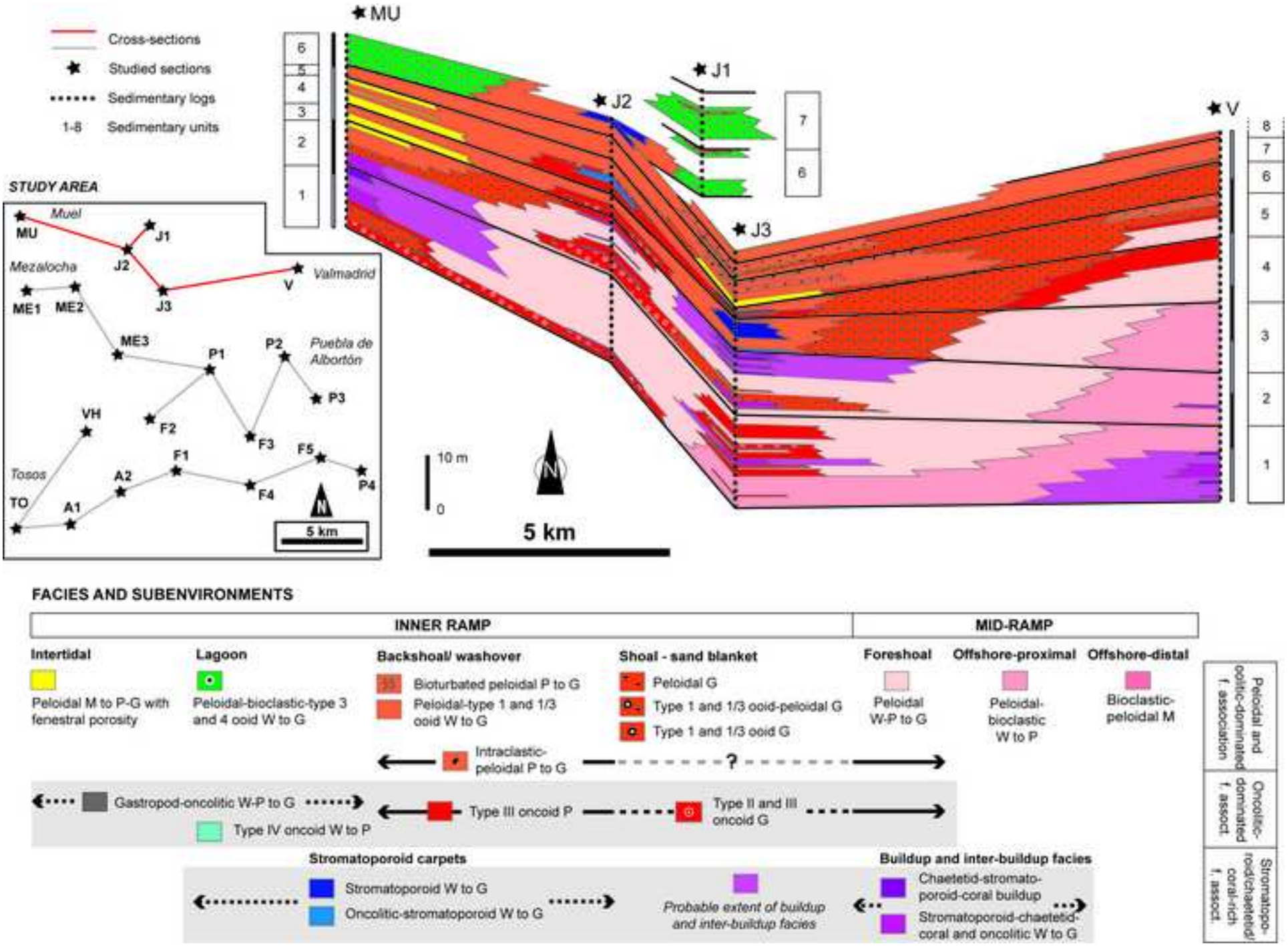

Figure 6

Click here to download high resolution image

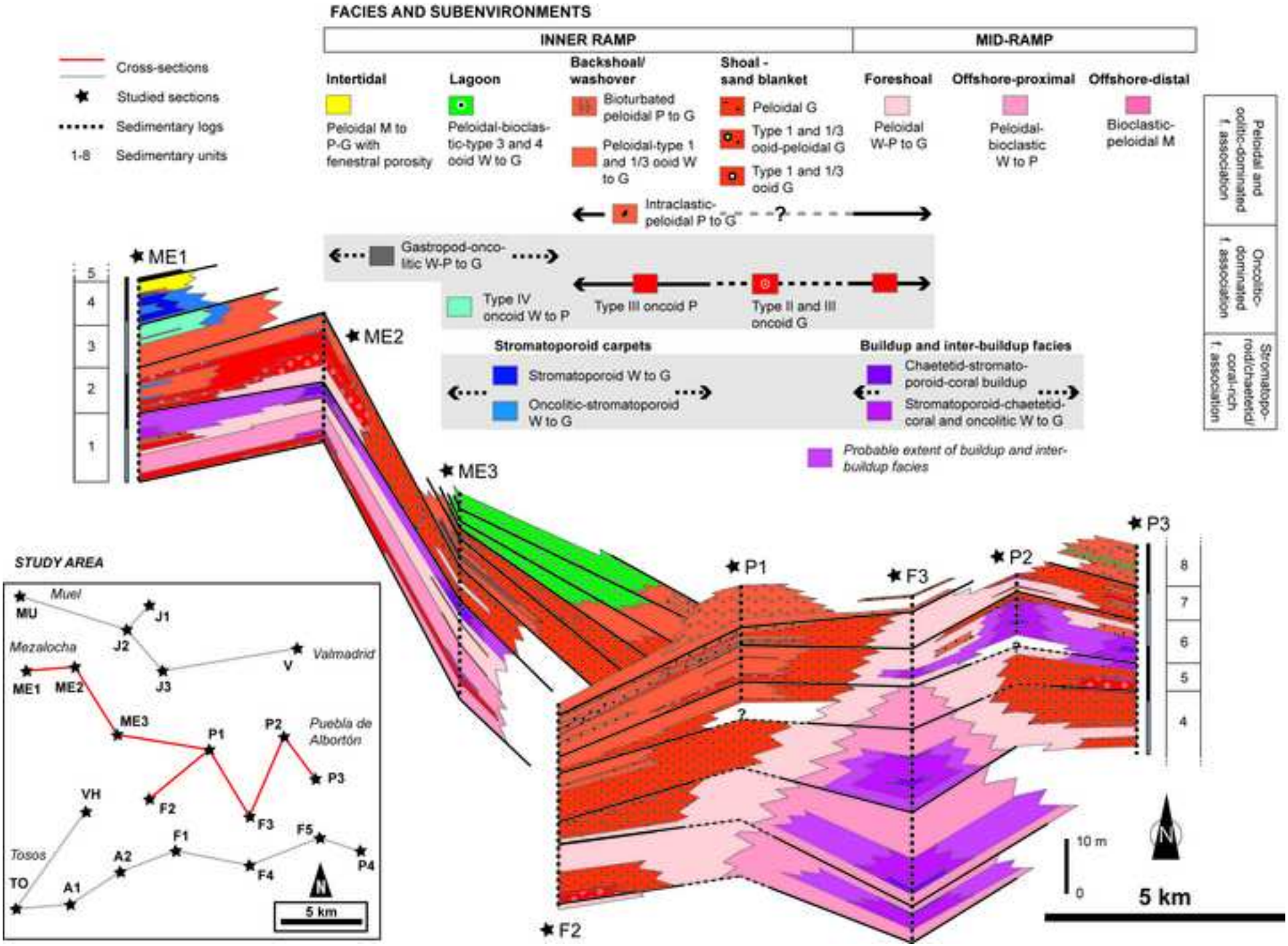

Figure 7

Click here to download high resolution image

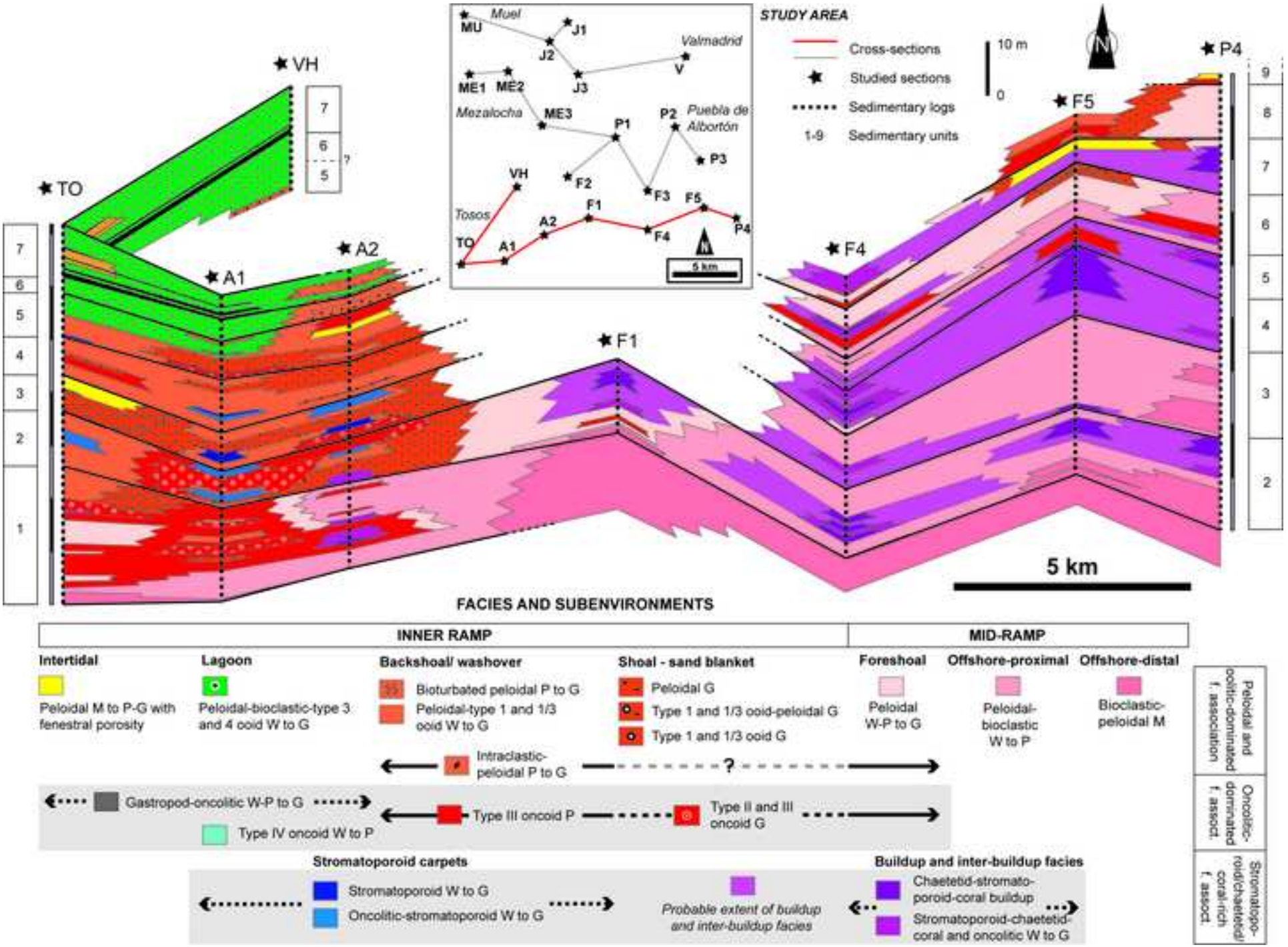

Figure 8

Click here to download high resolution image

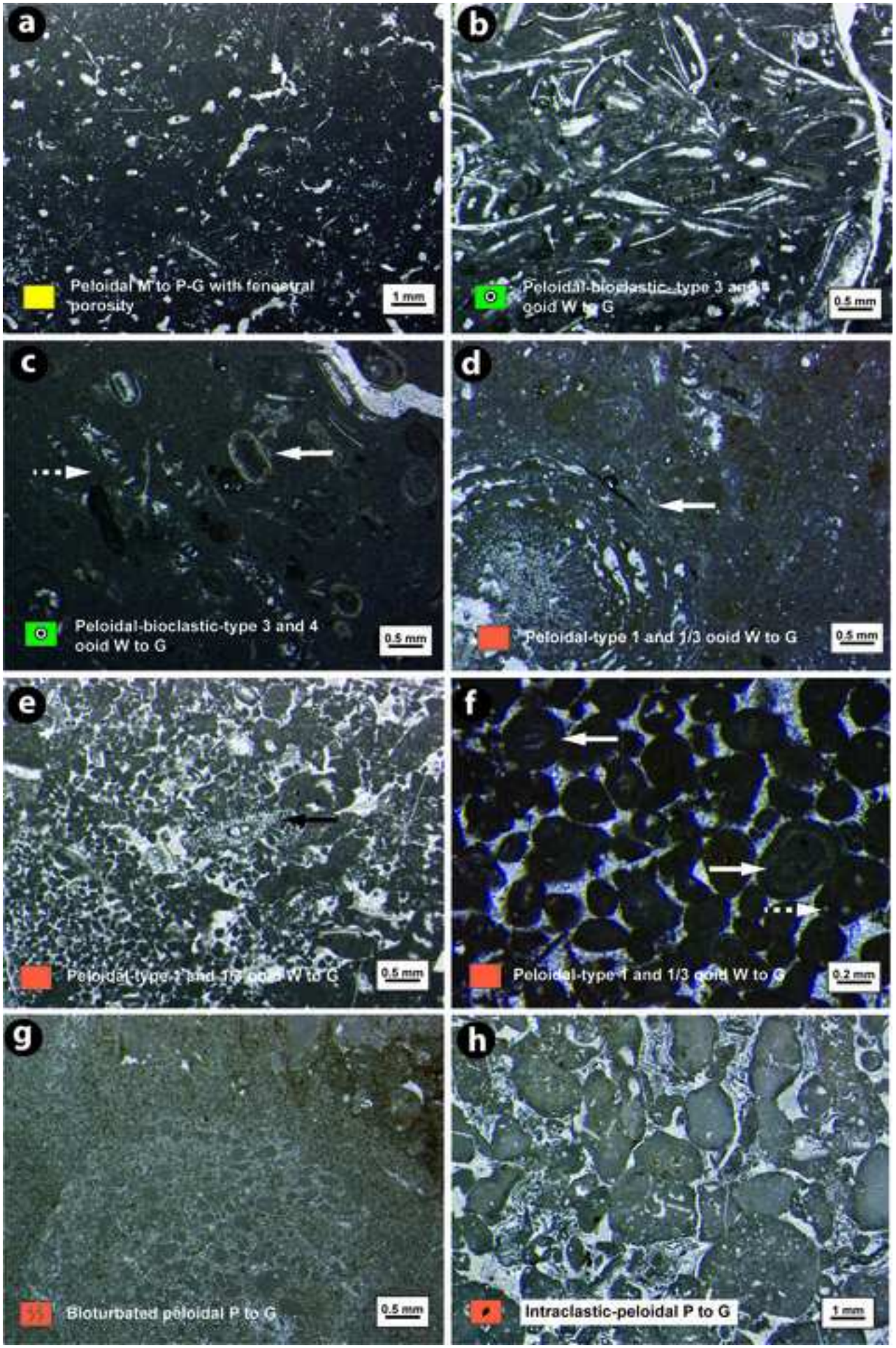

Figure 9

Click here to download high resolution image

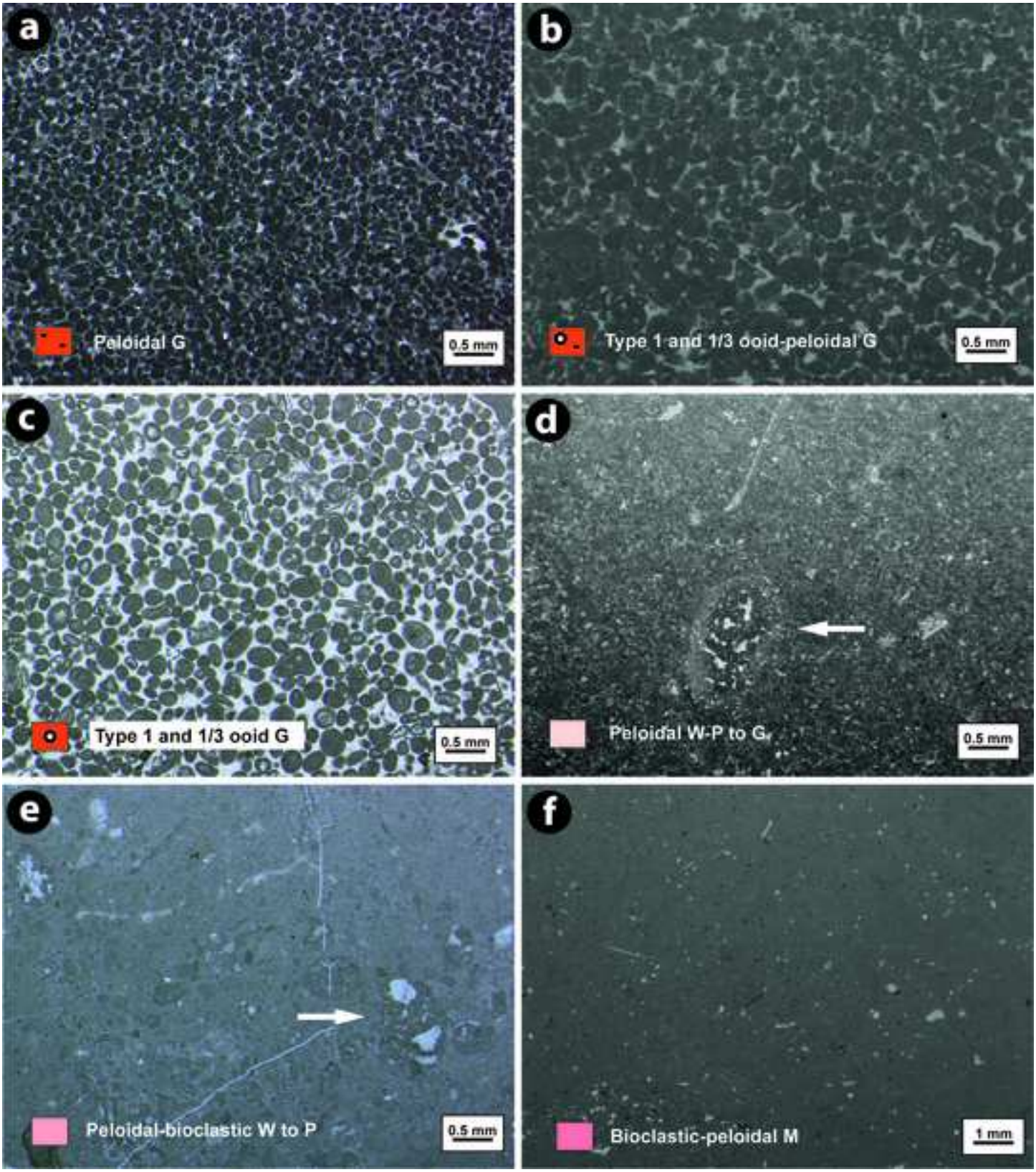

Figure 10

Click here to download high resolution image

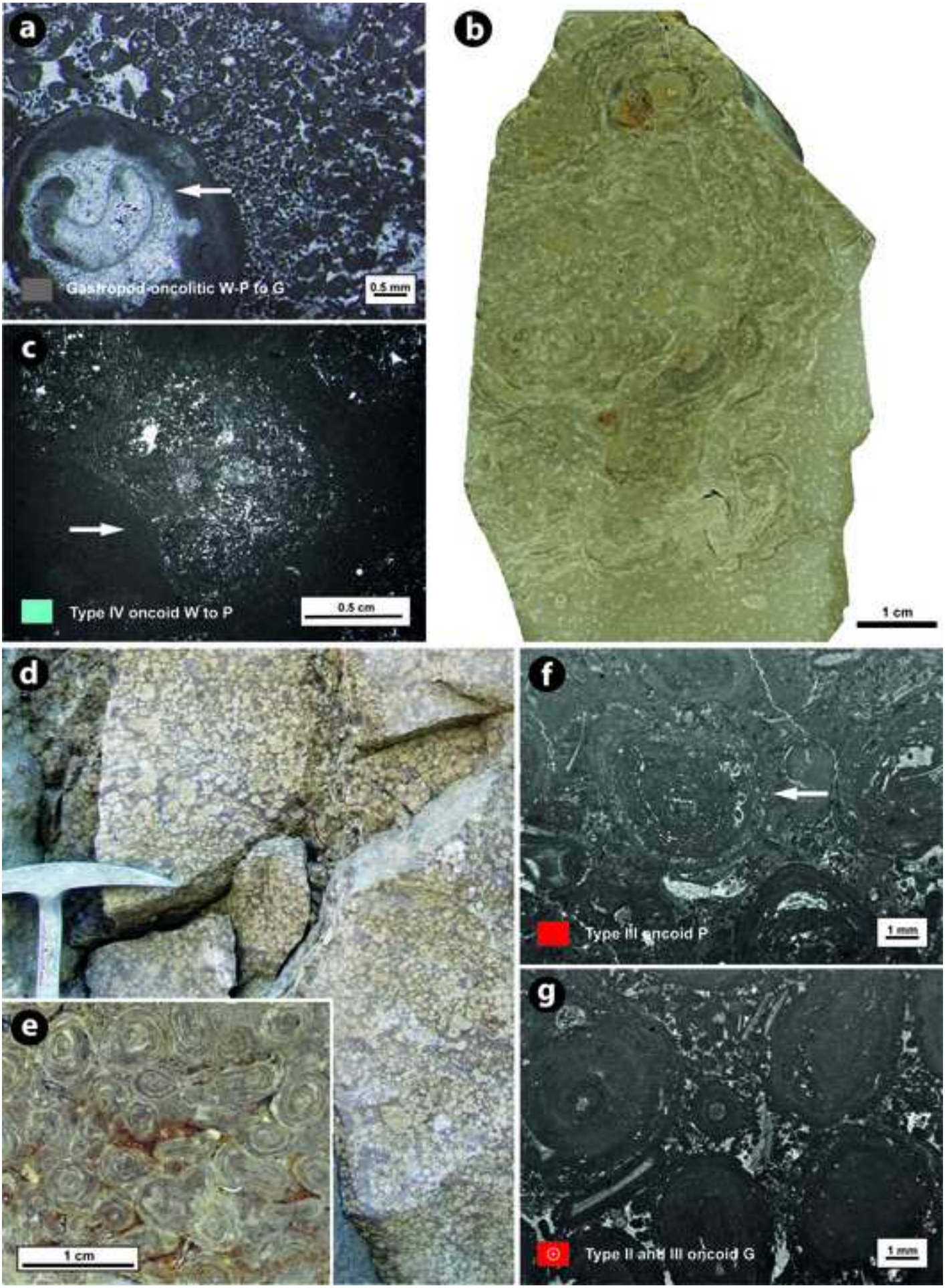

Figure 11

Click here to download high resolution image

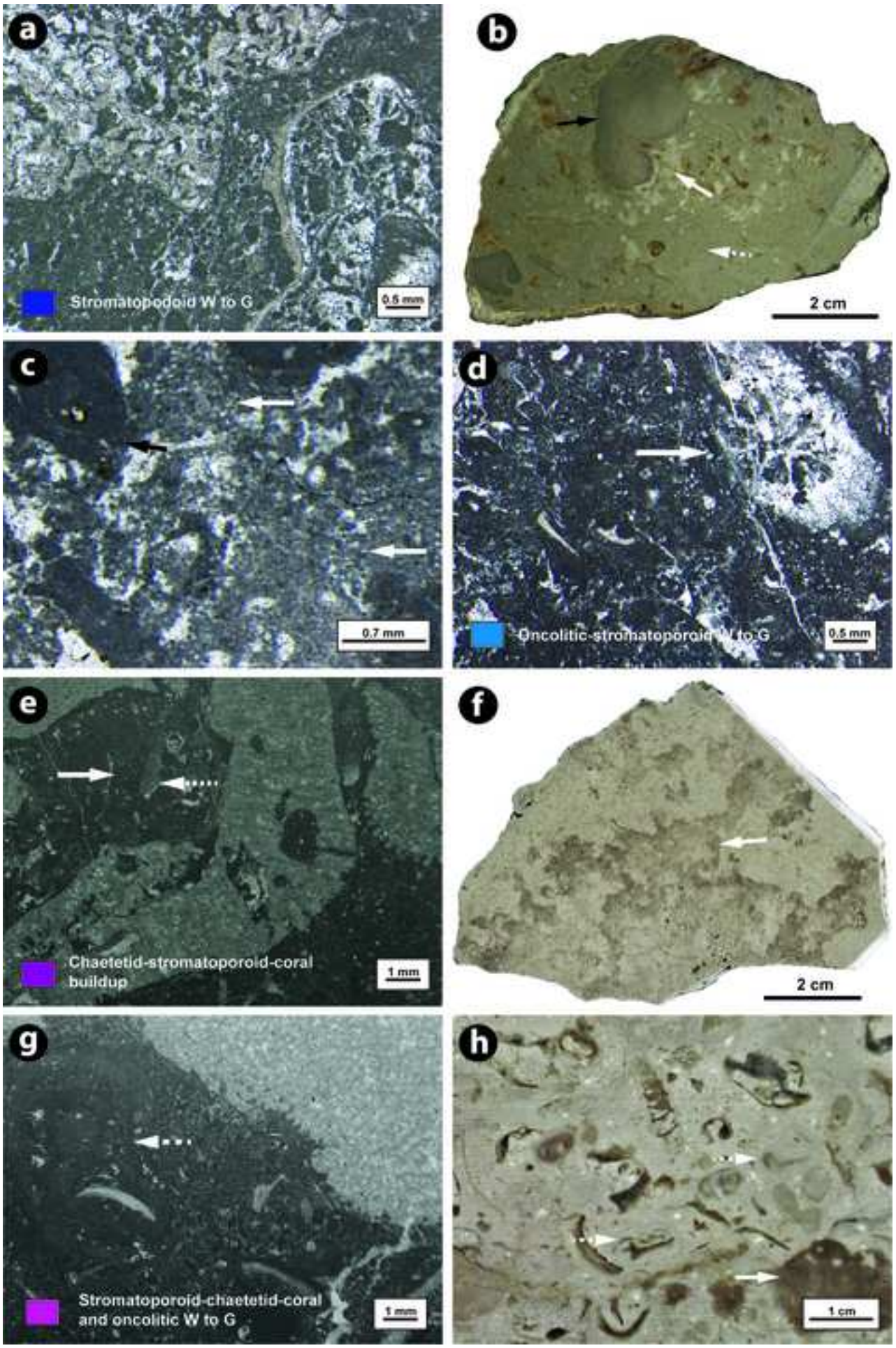

Figure 12

Click here to download high resolution image

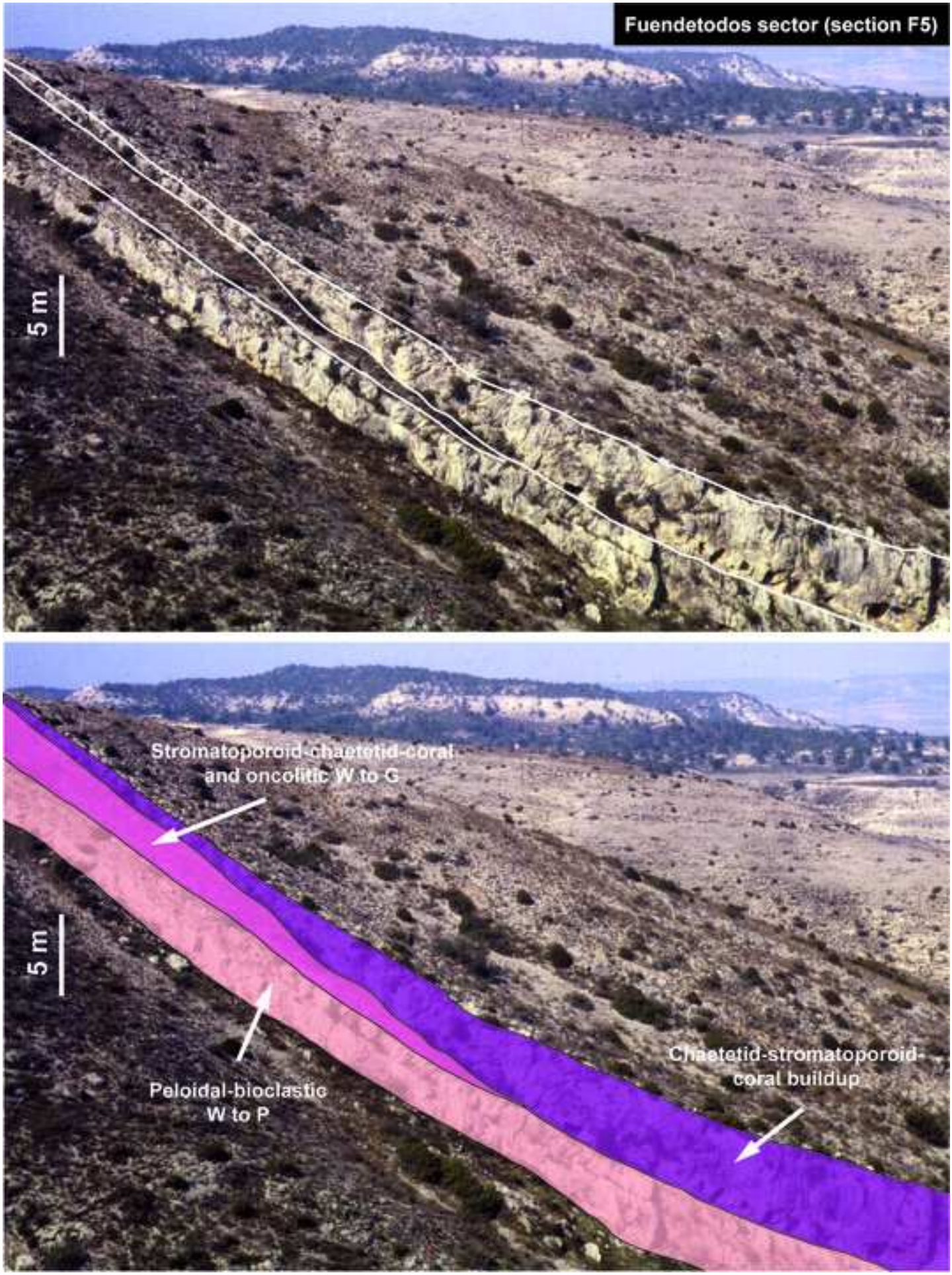

Figure 13

Click here to download high resolution image

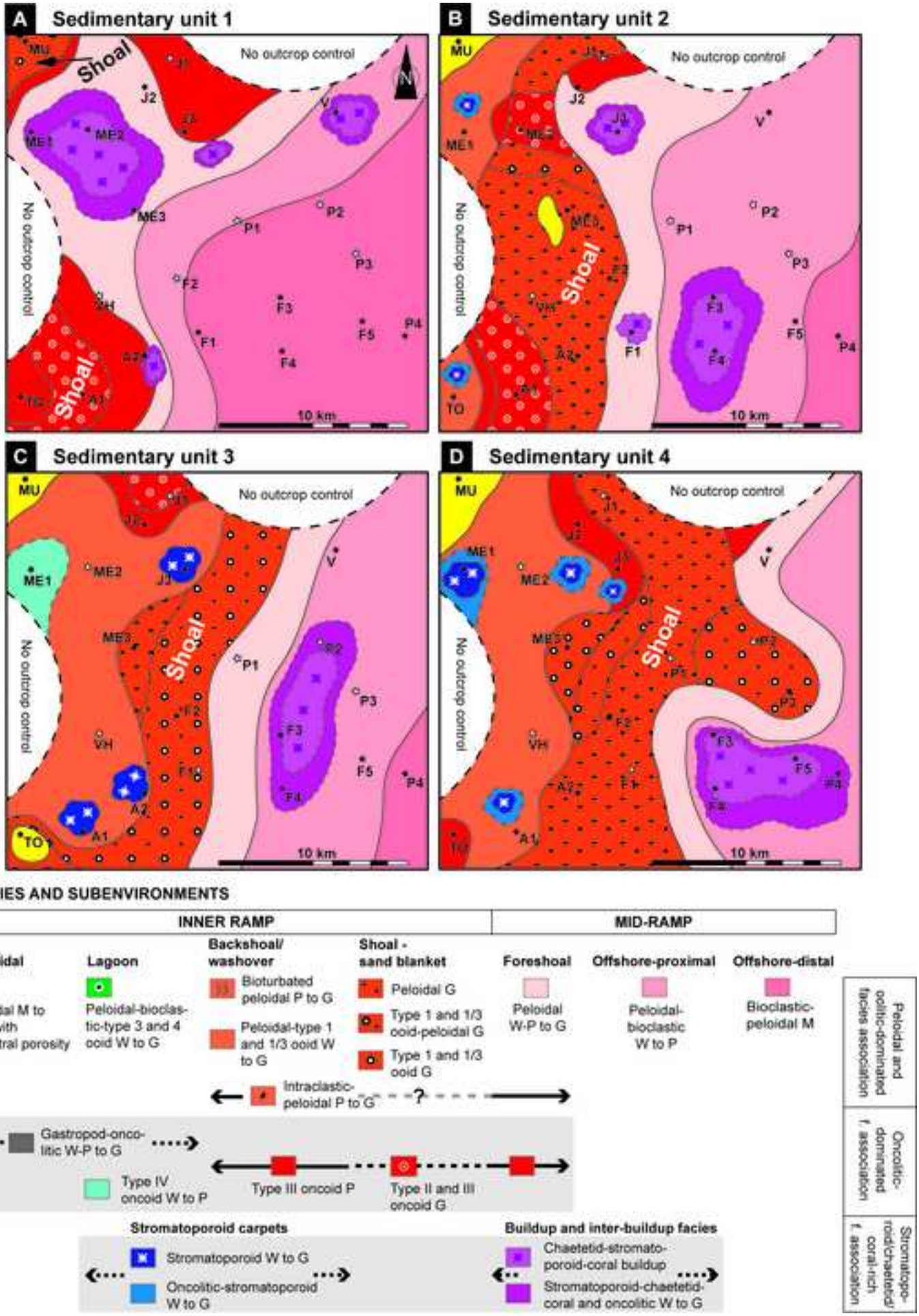

Figure 14

Click here to download high resolution image

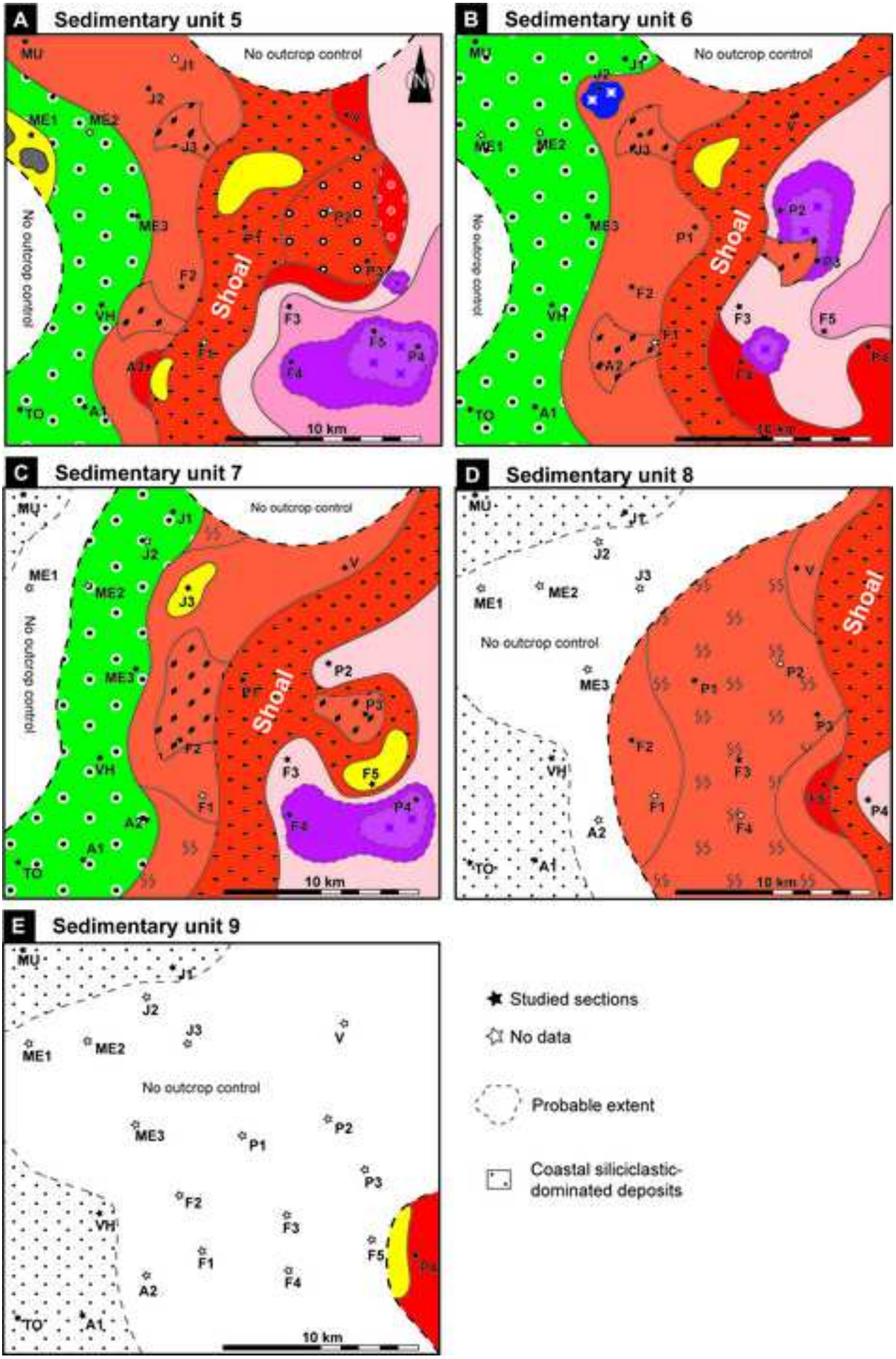

Figure 15

Click here to download high resolution image

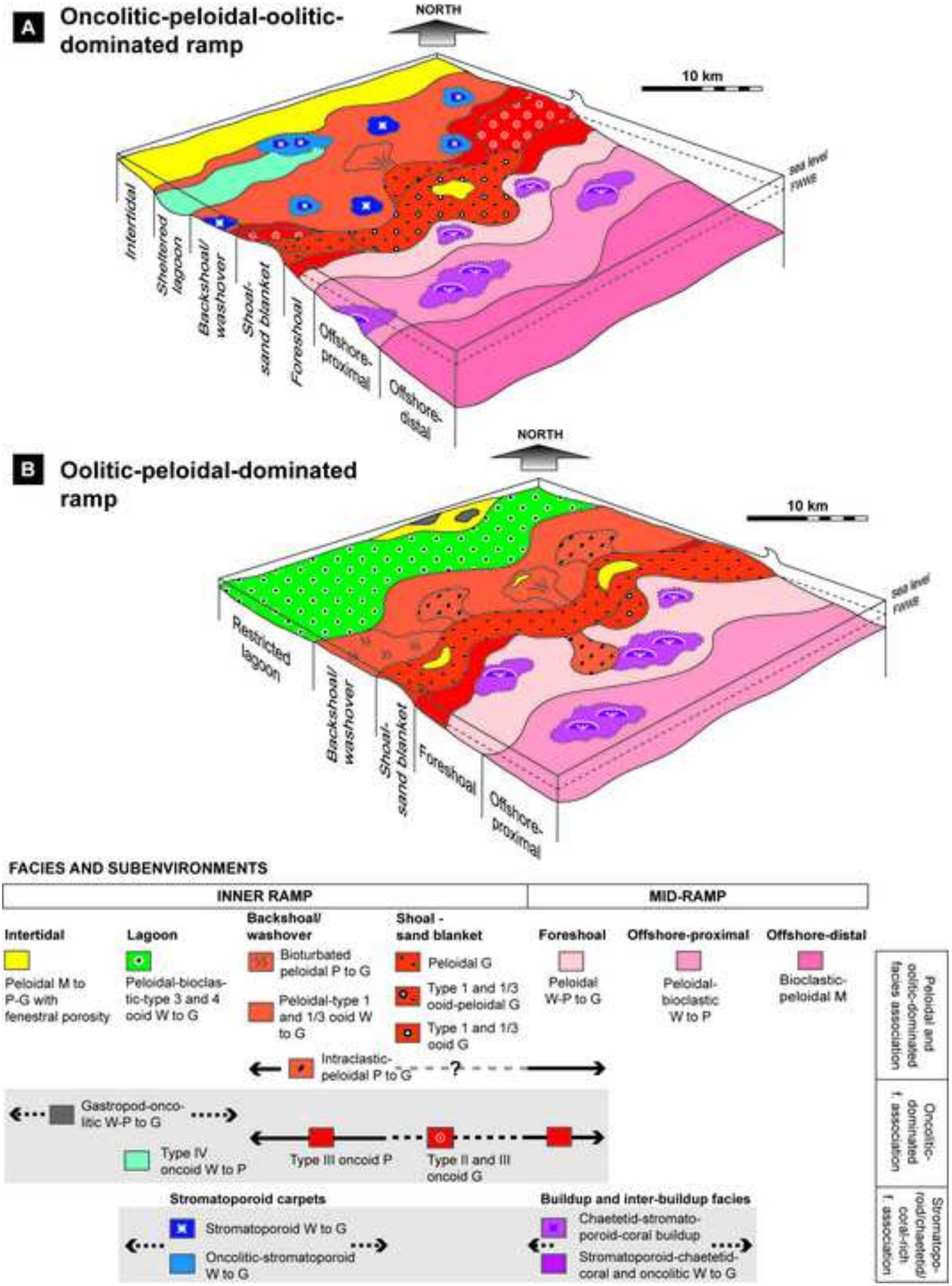

Figure 16

Click here to download high resolution image

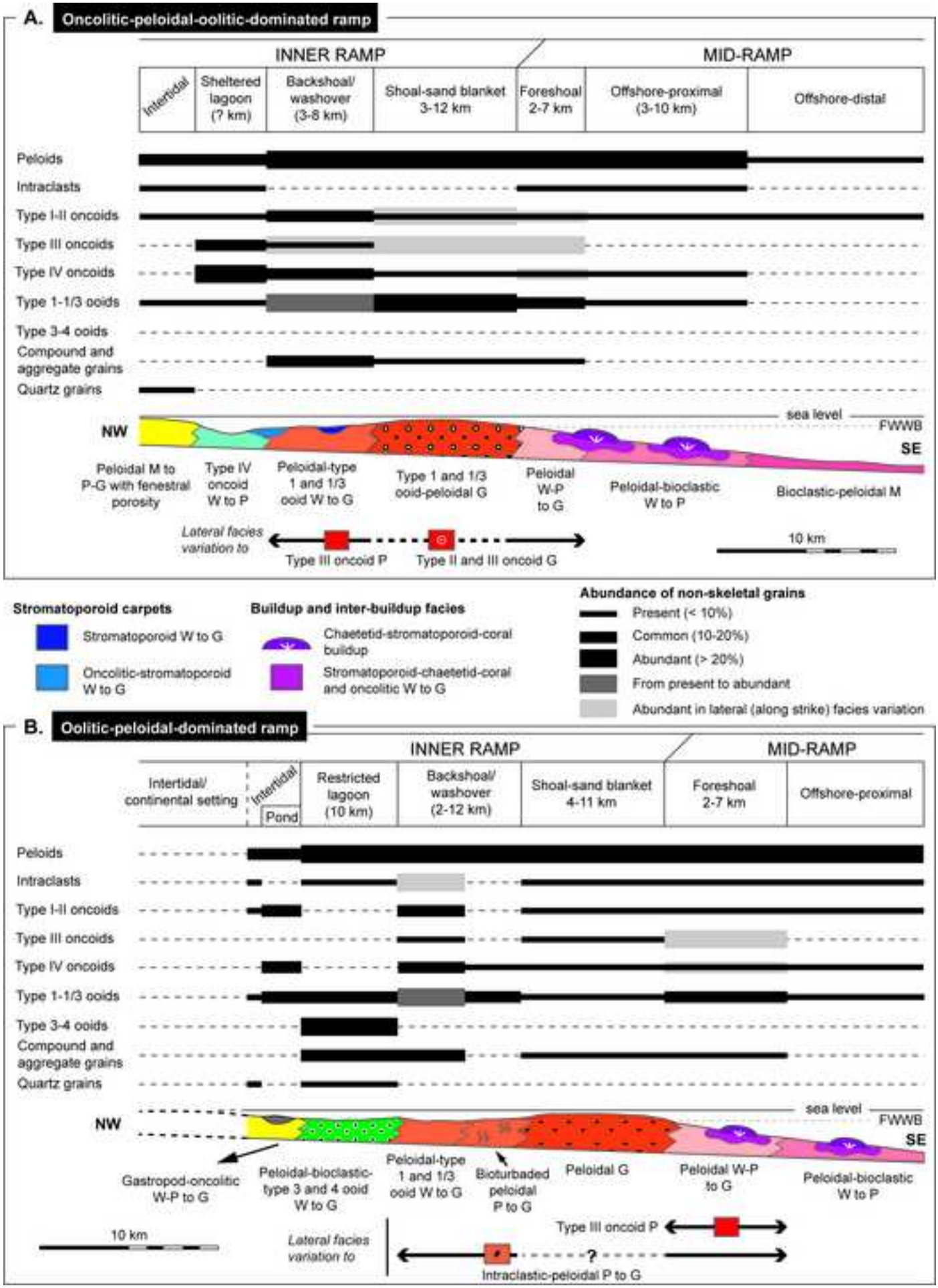

Figure 17

Click here to download high resolution image

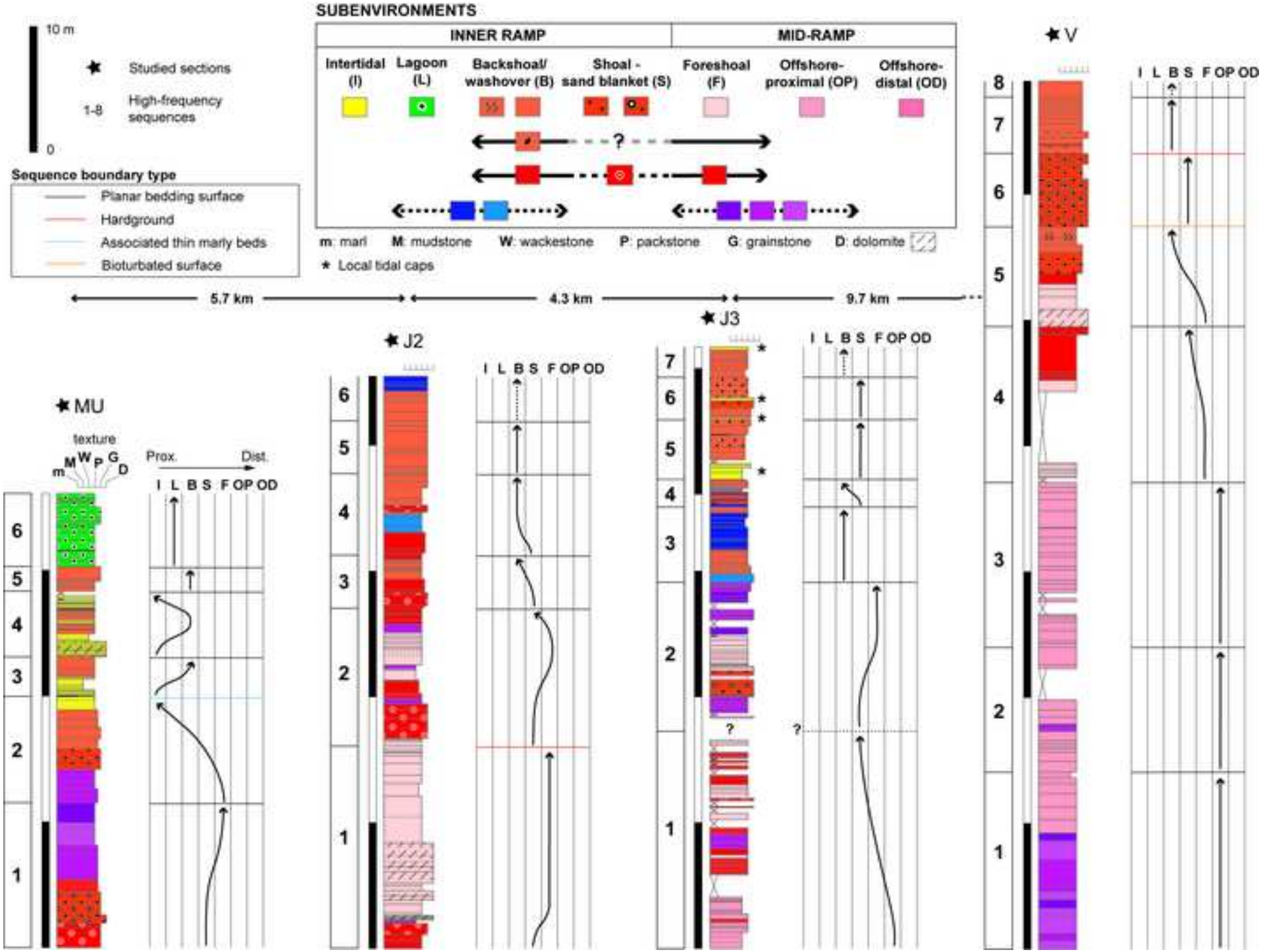

Figure 18

Click here to download high resolution image

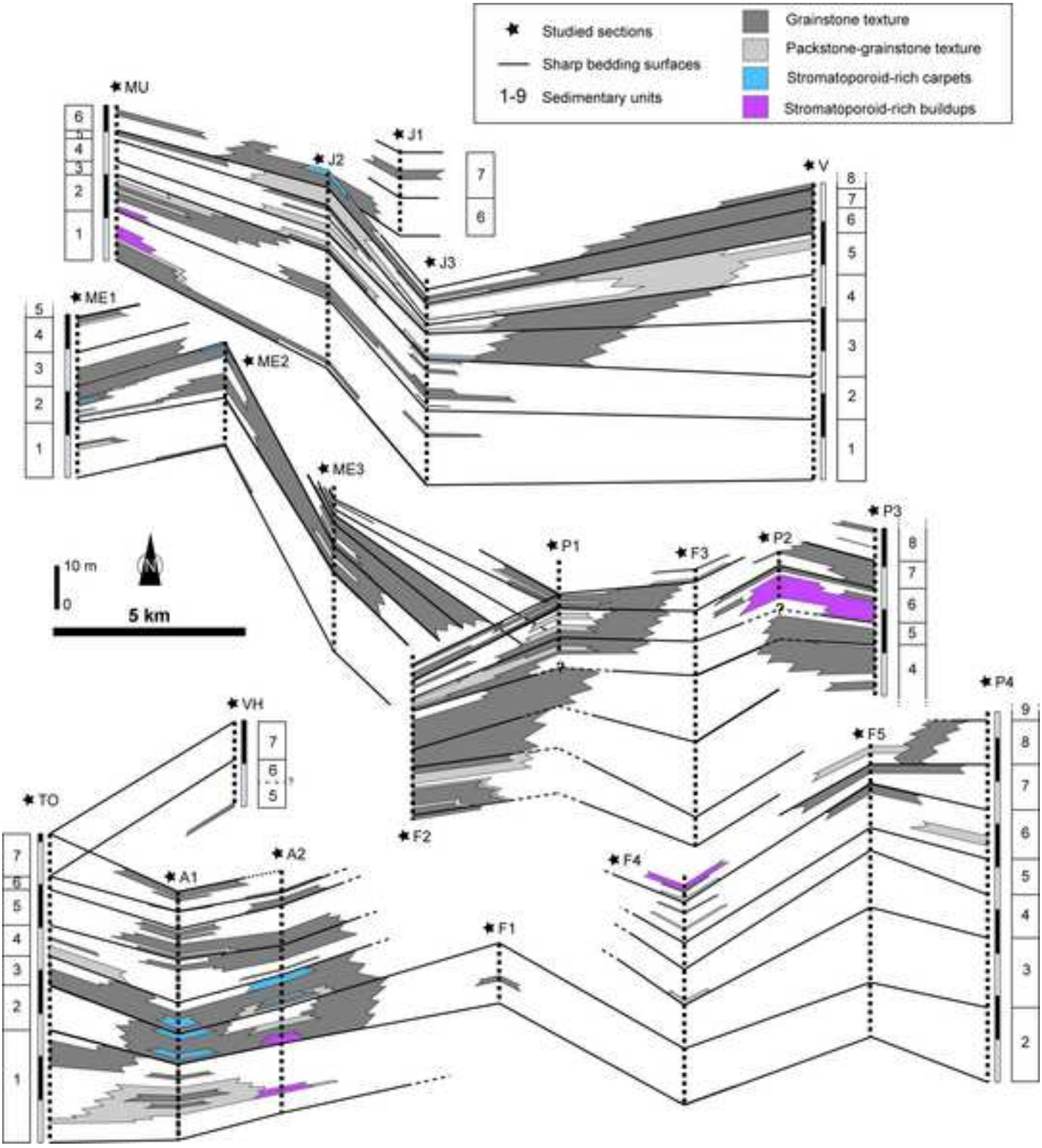

Table 1.

Non-skeletal grain	Type	Size and shape	Internal structure
Oncoid (Dahanayake, 1977, 1978)	I	Few millimetres; spherical to elliptical	Concentric and continuous micritic laminae
	II	Few millimetres to 1 cm; elliptical to sub-spherical	Micritic laminae with organism-bearing encrustations
	III	Few cms (up to 2 cm); spherical to irregular with wavy contours	Alternating micritic and organism-bearing laminae
	IV	Few mms to 7 cm; very irregular, lobate contours	Microbial meshwork, no lamination
Ooid (Strasser, 1986)	1	Up to 2 mm; spherical	Concentric thinly micritic laminae
	3		Fine-radial laminae
	1/3		Alternating fine-radial and micritic laminae
	4		Few thick-radial laminae
Peloid (Flügel, 2004)	Lithic	Variable in size; well-rounded to irregular	Micrite
	Microbial	Up to 600 µm; well-rounded	

Table 2

Facies / *Subenvironments*		Non-skeletal grains	Skeletal grains	Stratification and sedimentary structures
Peloidal and oolitic-dominated facies association				
Intertidal	**Peloidal M to P-G with fenestral porosity**	< 30% lithic peloids: poorly sorted (ø < 0.3 mm), irregular to well-rounded < 15% type 1 and 1/3 ooids (ø < 0.5 mm) < 10% type II oncoids: mm-sized, intraclastic nuclei, cortices with *Bacinella irregularis* Scarce intraclasts and sand-size quartz grains	< 7%: lituolids (2), miliolids (4), texturaliids (3, 5), bivalves and *Tubiphytes-Crescentiella*; scarce dasycladacean algae (4, 6, 8), gastropods, brachiopods, echinoderms, ostracods, *Cayeuxia-Ortonella*, involutiniids (3) and stromatoporoids	Tabular to irregular cm- to m-thick beds Fenestral porosity (10-25% of isolated fenestral pores ø < 2 mm), parallel fenestral laminites (< 3 mm thick); dome-like stromatolitic crusts with occasional mm- to cm-thick *Girvanella* and *Bacinella* encrusting laminae; local bioturbation
Restricted lagoon	**Peloidal-bioclastic-type 3 and 4 ooid W to G**	< 45% lithic peloids: well-sorted (ø < 0.2 mm), well-rounded < 45% type 3 and 4 ooids: poorly sorted (ø < 2 mm) and partly micritized, bioclastic and intraclastic (micritic) nuclei; common type 1/3 and 1/4 ooids, compound and aggregate ooids. Scarce intraclasts and sand-size quartz grains, and occasional glauconite	< 40%: highly micritized or ferruginous bivalves, lituolids (1, 3, 6, 8), gastropods, ostracods and echinoderms; scarce miliolids (1, 3), textulariids (5), dasycladacean algae (1, 3, 5), brachiopods and bony fish scales	Tabular dm- to m-thick beds, intercalated with marls; frequent ferruginization Frequent bioturbation (*Thalassinoides* traces, filled by pellets); cm-thick bioclastic laminae with normal gradation and parallel lamination
Backshoal/washover	**Peloidal-type 1 and 1/3 ooid W to G**	< 75% lithic peloids: poorly to well-sorted (ø < 0.3 mm), irregular to well-rounded < 50% type 1 and 1/3 ooids: ø < 2 mm, bioclastic and intraclastic (micrite) nuclei, common compound and aggregate ooids < 20% type II and IV oncoids: ø < 2 cm, bioclasts, intraclasts and aggregate grains in the nuclei; type IV oncoids with *Lithocodium aggregatum*, *Bacinella*, *Girvanella*, *Cayeuxia-Ortonella*, *Troglotella*; common compound and aggregate oncoids; scarce type I and III oncoids	< 20%: commonly micritized: lituolids (1, 5, 6), textulariids (2, 3, 4, 5), miliolids (3, 4), brachiopods, bivalves, echinoderms, gastropods and dasycladacean algae (4, 6, 8); scarce *Tubiphytes*, rotaliids, serpulids, *Cayeuxia-Ortonella*, involutiniids (1, 3), ostracods, corals (1, 2), chaetetids (1, 3), stromatoporoids (3), *Thaumatoporella parvovesiculifera* and bryozoans	Tabular to irregular dm- to m-thick beds Local parallel- and cross-lamination; mm- to cm-thick oncolitic, skeletal and oolitic laminae with normal gradation; common bioturbation
	Bioturbated peloidal P to G	< 65% lithic peloids: well-sorted (ø < 0.3 mm), rounded to irregular < 25% type 1/3 ooids: ø < 0.2 mm, sometimes ferruginized; scarce type 1, 4 and 1/4 ooids < 12% type IV oncoids: mm-sized Local ferruginized intraclasts (micritic facies with bioclasts).	< 15%: micritized lituolids (1, 6), gastropods, echinoderms, bivalves and miliolids (3); scarce brachiopods, ostracods, textulariids (5), dasycladacean algae (6), corals (locally in-situ), bryozoans and serpulids	Tabular dm-thick beds; frequent ferruginization Intense burrowing (*Thalassinoides* traces); local parallel lamination
Shoal-sand blanket	**Peloidal G**	< 75% lithic peloids: well-sorted (ø < 0.2 mm) and rounded < 15% type 1 and 1/3 ooids: poorly to well-sorted (ø < 2 mm), bioclastic and intraclastic (micritic) nuclei < 15% type I, II, III and IV oncoids: ø < 1 cm, spherical to irregular, bioclasts, intraclasts (micrite) and aggregate grains in the nuclei; occasional compound oncoids Scarce intraclasts (micritic and grain-supported facies with peloids, ooids and bioclasts) and aggregate grains	< 10%: textulariids (3, 4, 5), miliolids (3, 4), lituolids (5, 6), echinoderms, bivalves, brachiopods and gastropods; scarce stromatoporoid and coral fragments, *Tubiphytes*, *Cayeuxia-Ortonella*, involutiniids, dasycladacean algae and *Thaumatoporella*	Tabular to irregular dm- to m-thick beds Common parallel lamination; local bioturbation and cm-thick oncolitic laminae with normal gradation
	Type 1 and 1/3 ooid-peloidal G	< 40% lithic peloids: well-sorted (ø < 0.2 mm), rounded < 40% type 1 and 1/3 ooids: poorly sorted (ø < 2 mm), ovoid to spherical, bioclastic and intraclastic (micrite) nuclei; common aggregate ooids < 10% type I, II and IV oncoids: ø < 1 cm, spherical to irregular, bioclasts and aggregate grains in the nuclei; type IV oncoids with *Bacinella*, *Girvanella*, *Troglotella*; common compound oncoids	< 5%: lituolids (5), miliolids (3), textulariids (5), brachiopods, gastropods and bivalves; scarce corals, stromatoporoids, serpulids, *Tubiphytes*, *Cayeuxia-Ortonella* and dasycladacean algae	Tabular to irregular dm- to m-thick beds Local bioturbation and parallel- and cross-lamination
	Type 1 and 1/3 ooid G	< 60% type 1 and 1/3 ooids: well-sorted (ø < 0.5 mm), ovoid to spherical, bioclastic and intraclastic (micrite) nuclei; occasional type 1/4 ooids < 20% lithic peloids: well-sorted (ø < 0.2 mm) and rounded < 8% type I, II and IV oncoids: well-sorted (ø < 0.5 cm) and spherical, bioclastic nuclei Scarce intraclasts (micritic facies with peloids, ooids, bioclasts and fine quartz sand)	< 5%: brachiopods, lituolids, miliolids (3) and gastropods; scarce echinoderms, dasycladacean algae, texturaliids and *Troglotella*	Tabular to irregular cm- to m-thick beds Local bioturbation

Foreshoal	**Peloidal** **W-P to G**	< 70% lithic peloids: poorly to well-sorted (ø < 0.2 mm) < 35% type 1 and 1/3 ooids: well-sorted (ø < 2 mm), bioclastic and intraclastic (micrite) nuclei; scarce compound and aggregate ooids < 20% type I, II, III and IV oncoids: ø < 2 cm, spherical to irregular, bioclastic and intraclastic (grain-supported facies with peloids, ooids and bioclasts) nuclei, cortices with *Lithocodium, Bacinella*, *Cayeuxia-Ortonella* and *Troglotella*, and serpulids; occasional compound oncoids Scarce intraclasts (micrite and grain-supported facies with peloids, ooids and bioclasts)	< 20%: lituolids (6), echinoderms, brachiopods, bivalves (1, 2) and miliolids (3); scarce gastropods, textulariids (3, 4, 5), rotaliids, involutiniids, *Tubiphytes*, stromatoporoids (3), corals (locally in-situ), chaetetids and dasycladacean algae (2, 6, 8)	Tabular to irregular dm- to m-thick beds Common bioturbation; local parallel lamination
Storm lobes in backshoal and foreshoal	**Intraclastic-peloidal** **P to G**	< 45% intraclasts and < 40% lithic peloids: poorly sorted (mm to cm in size) and poorly rounded fragments of micritic facies (with bioclasts and fine quartz sand) and grain-supported facies (ooids, peloids and bioclasts), grading into rounded poorly to well-sorted lithic peloids (ø < 0.3 mm) < 14% type IV oncoids: small irregular	< 15%: mm to cm in size, commonly micritized, gastropods, bivalves, *Cayeuxia-Ortonella*, brachiopods, miliolids (2, 3), lituolids (2, 6) and texturaliids (3, 4, 5); scarce dasycladacean algae (6, 8), echinoderms, corals, involutiniids (3), ostracods and bryozoans	Tabular to irregular dm-thick beds Common mm- to cm-thick bioclastic and intraclastic laminae, and local intraclastic mm-thick graded laminae; local bioturbation
Offshore-proximal	**Peloidal-bioclastic** **W to P**	< 70% lithic peloids: poorly to well-sorted (ø < 0.3 mm) and rounded; local microbial peloids (ø = 100 µm in mean diameter) < 10% type I, II and IV oncoids: ø < 1cm, spherical to irregular, bioclastic and intraclastic (grain-supported facies with peloids, ooids and bioclasts) nuclei; type II and IV oncoids with cortices including *Bacinella* and *Girvanella*, serpulids, foraminifers and *Tubiphytes*; local type III oncoids, compound and aggregate oncoids Scarce type 1 and 1/3 ooids, well-sorted (ø < 2 mm), ovoid to spherical, bioclastic nuclei; and intraclasts (micritic facies)	< 20%: mm- to cm-sized, lituolids (4, 6, 7), corals (locally in-situ), echinoderms, serpulids (1, 2), chaetetids, bivalves, gastropods and brachiopods; scarce stromatoporoids (3), sponges, miliolids (2), textulariids (5, 6), involutiniids (2), lageniids (1, 2, 3), *Tubiphytes*, *Lithocodium*, dasycladacean algae (8) and belemnites	Tabular to irregular dm- to m-thick beds Frequent bioturbation (*Chondrites* and *Planolites* traces); local cm-thick oncolitic laminae
Offshore-distal	**Bioclastic-peloidal** **M**	< 8% lithic peloids: poorly sorted (ø < 0.1 mm), irregular to well-rounded Scarce type I and II oncoids: mm-sized, bioclastic nuclei; cortices with occasional serpulids; local compound oncoids Occasional intraclasts and fine quartz sand	< 8%: lituolids (4, 6), echinoderms, bivalves, gastropods and sponges; scarce serpulids (1, 2), brachiopods, miliolids, texturaliids (1, 3, 6), lageniids (2, 3), rotaliids, involutina (2), *Tubiphytes*, *Troglotella*, *Lithocodium*, dasycladacean algae (8) and reefal debris (stromatoporoids, chaetetids and corals)	Tabular dm- to m-thick beds Frequent bioturbation (*Chondrites* and *Planolites* traces)
Oncolitic-dominated facies association				
Pond/restricted lagoon	**Gastropod-oncolitic** **W-P to G**	< 30% type I, II and IV oncoids: ø < 1 cm, spherical to irregular, bioclastic nuclei; type IV oncoids with *Bacinella* < 30% type 1 and 1/3 ooids: ø < 2 mm, ovoid to spherical, bioclastic and intraclastic (micrite) nuclei < 20% lithic peloids: ø < 0.2 mm, irregular to well-rounded	< 20%: broken and whole gastropods; small skeletal grains, commonly micritized, of bivalves, lituolids (1, 6), miliolids (3) and texturaliids (5); scarce dasycladacean algae (7), echinoderms, brachiopods, *Thaumatoporella*, sponges, *Cayeuxia-Ortonella*, *Tubiphytes* and involutiniids (1)	Tabular cm- to dm-thick beds, locally intercalated with cm-thick marly beds Components accumulated in cm-thick laminae; local bioturbation
Sheltered lagoon	**Type IV oncoid** **W to P**	< 40% type IV oncoids: ø < 7 cm, irregular, bioclastic nuclei, thick crusts with *Bacinella*, *Lithocodium*, *Cayeuxia-Ortonella*, *Girvanella*, *Thaumatoporella* and sponges, sometimes forming the entire cortex; common type III oncoids; local mm-sized type I and II oncoids < 30% lithic peloids: well-sorted (ø < 0.2 mm), local microbial peloids Scarce type 1 and 1/3 ooids (ø < 0.1 mm) and intraclasts (micritic and grain-supported facies with peloids)	< 15%: commonly micritized, lituolids (1, 5, 6), miliolids (4), texturaliids (3, 5), bivalves, echinoderms and brachiopods; scarce gastropods, dasycladacean algae (3, 6, 8), rotaliids, involutiniids (3), *Cayeuxia-Ortonella*, *Tubiphytes*, ostracods, sponges, stromatoporoids and corals (locally in-situ)	Tabular dm- to m-thick beds Local cm-thick oncolitic laminae; bioturbation

Backshoal and foreshoal	**Type III oncoid P**	20-60% type III oncoids: ø < 2cm, occasionally < 4 cm, spherical to irregular, with bioclastic and intraclastic (mud- and grain-supported facies with peloids, ooids and bioclasts) nuclei, cortices with *Bacinella*, *Lithocodium*, *Troglotella*, *Girvanella* and *Cayeuxia-Ortonella*, and sponges, foraminifera, serpulids and *Tubiphytes*; common type II, IV and compound oncoids. < 45% microbial and poorly to well-sorted lithic peloids (ø < 0.3 mm) < 30% type 1 and 1/3 ooids: poorly sorted (ø < 2 mm)	< 20 % lituolids (1, 4, 5, 6), miliolids (3, 4), textulariids (2, 3, 5, 6), echinoderms, gastropods, mm- to cm-sized fragments of bivalves (2) and brachiopods, and stromatoporoids (3, 6) and chaetetids (4) in mm-to cm-sized fragments and in-situ; scarce serpulids (1, 2), dasycladacean algae (4), *Tubiphytes*, sponges, bryozoan, *Cayeuxia-Ortonella*, involutiniids (2, 3), rotaliids and coral fragments	Tabular to irregular dm- to m-thick beds Local mm- to cm-thick oncolitic laminae; local bioturbation and borings in oncoids and stromatoporoids
Shoal-sand blanket	**Type II and III oncoid G**	20-60% type II and III oncoids: ø < 2cm, spherical to irregular, with bioclastic and intraclastic (grain-supported facies with peloids, ooids and bioclasts) nuclei, cortices with *Bacinella*, *Lithocodium*, *Troglotella*, *Thaumatoporella*, *Girvanella* and *Cayeuxia-Ortonella*, and serpulids; common type I and compound oncoids < 30% poorly sorted lithic peloids (ø < 0.3 mm) < 20% type 1 and 1/3 ooids: poorly sorted (ø < 2 mm)	< 10% lituolids (5), echinoderms, bivalves and mm- to cm-sized fragments of brachiopods; scarce miliolids (3), texturaliids (5), gastropods, serpulids (1, 2), *Tubiphytes*, dasycladacean algae (6), stromatoporoids (1, 3, 6), chaetetids (1, 4), corals, involutiniids (3) and *Cayeuxia-Ortonella*	Tabular to irregular dm- to m-thick beds
Stromatoporoid/chaetetid/coral-rich facies association				
Stromatoporoid carpets				
Sheltered lagoon to backshoal	**Stromatoporoid W to G**	< 20% microbial and lithic peloids < 10% type I and II oncoids: ø < 1 cm, bioclastic nuclei; type II oncoids with *Lithocodium*, *Bacinella*, *Thaumatoporella* and *Girvanella* Scarce type 1 and 1/3 ooids (ø < 1 mm)	< 40% cm-sized and in-situ stromatoporoids (1, 2, 3, 6), and lower proportion of chaetetids (1, 6) and corals (2); common *Tubiphytes* encrustations < 15% fine-grained skeletal fraction: mainly bivalves, brachiopods, echinoderms, lituolids (5), miliolids (3, 4), textulariids (4, 5) and dasycladacean algae (5, 6, 8)	Tabular to irregular dm- to m-thick beds Bioclastic mm- to cm-thick laminae; bivalve borings on stromatoporoids and bioturbation
	Oncolitic-stromatoporoid W to G	< 20% type I, II, III and IV oncoids: ø < 3 cm, well-rounded to irregular, bioclastic and intraclastic (micrite) nuclei; III and IV oncoids with *Lithocodium*, *Bacinella*, *Girvanella*, *Cayeuxia-Ortonella* and *Troglotella* < 10% lithic and microbial peloids: ø < 0.2 mm, irregular to well-rounded Scarce type 1 and 1/3 ooids (ø < 2 mm)	< 40% cm-sized stromatoporoids and corals as in stromatoporoid W to G < 15% fine-grained skeletal fraction: mainly *Tubiphytes*, lituolids (1, 5), miliolids (3, 4), textulariids (3, 4, 5), bivalves, gastropods, echinoderms and brachiopods	Tabular to irregular dm- to m-thick beds Components accumulated in mm- to cm-thick laminae; common bioturbation and local bivalve borings on stromatoporoids
Buildup and inter-buildup facies				
Foreshoal to offshore-proximal	**Chaetetid-stromatoporoid-coral buildup**	< 40% microbial and poorly sorted and rounded lithic peloids, (ø < 0.2 mm) < 10% type I and II oncoids: ø < 1 cm, bioclastic nuclei; type II oncoids with *Bacinella*, *Lithocodium* and *Troglotella*, and other encrusters (serpulids) Scarce type III and IV oncoids	< 40% primary reef builders: cm-sized and in-situ chaetetids (1, 2, 4, 5, 6) and stromatoporoids (1, 3, 4, 6); corals (1, 2) are locally abundant < 10% secondary reef builders: dense micritic to local peloidal microbial crust, with encrusters around the primary reef builders: serpulids, foraminifera, sponges, *Cayeuxia*, *Girvanella*, *Thaumatoporella*, *Bacinella*, *Tubiphytes*, *Troglotella* and *Lithocodium* < 10% fine-grained skeletal fraction: mm- to cm-sized brachiopods, bivalves, echinoderms, serpulids (1), *Cayeuxia-Ortonella* and sponges	Up to 8 m high with low step margins Bivalve and sponge borings on chaetetids, corals and stromatoporoids, filled by mud-supported sediment with microbial peloids; inter-growth cavities filled by mud-supported sediment with microbial peloids, bioclasts, microbial crust fragments and oncoids; bioturbation (grain-supported facies)
	Stromatoporoid-chaetetid-coral and oncolitic W to G	< 30% type II, III and IV oncoids: ø < 2 cm, spherical to irregular; cortices with *Bacinella*, *Girvanella*, *Lithocodium*, *Thaumatoporella*, *Troglotella* and *Cayeuxia-Ortonella*, and serpulids and gastropods; common compound and aggregate oncoids < 40% microbial and poorly sorted and rounded lithic peloids (ø < 0.2 mm) Scarce type 1 and 1/3 ooids (ø < 2 mm)	< 25% mm- to cm-sized stromatoporoids (1, 3, 5, 6) and chaetetids (1, 5); corals (2) are locally abundant < 20% fine-grained skeletal fraction: mm- to cm-sized echinoderms, bivalves, brachiopods and gastropods; scarce sponges, serpulids (1, 2), lituolids (4), miliolids (2), textulariids (3, 5, 6), *Tubiphytes*, *Thaumatoporella*, *Cayeuxia-Ortonella* and dasycladacean algae	Tabular to irregular dm- to m-thick beds Bivalve and serpulid borings on stromatoporoids and chaetetids; local serpulid borings in oncoids and cm-thick oncolitic laminae; bioturbation

Table 3.

Skeletal components

Foraminifera

Lituolidae
[1] *Alveosepta jaccardi*
[2] *Ammobaculites* sp.
[3] *Choffatella*
[4] *Everticyclammina*
[5] *Labyrinthina mirabilis*
[6] *Pseudocyclammina* sp.
[7] *Rectocyclammina*
[8] *Redmondellina powersi*

Miliolidae
[1] *Charentia evoluta*
[2] *Nautiloculina circularis*
[3] *Nautiloculina oolithica*
[4] *Quinqueloculina* sp.

Textulariidae
[1] *Bositra buchi*
[2] *Conicokurnubia*
[3] *Kurnubia jurassica*
[4] *Kurnubia palastinensis*
[5] *Redmondoides lugeoni*
[6] *Siphovalvulina*

Rotalidae (*Mohlerina basiliensis)*

Lagenidae
[1] *Dentalina*
[2] *Lenticulina sublenticularis*
[3] *Nodosaria* sp.

Involutina
[1] *Andesenolina*
[2] *Protopeneroplis striata*
[3] *Trocholina alpina*

Chlorophyta

Dasycladacean algae
[1] *Acicularia*
[2] *Campbeliella striata*
[3] *Clypeina* sp.
[4] *Clypeina jurassica*
[5] *Pseudoclypeina distomensis*
[6] *Salpingoporella annulata*
[7] *Salpingoporella dinarica*
[8] *Salpingoporella pygmaea*

Reefal components

Chaetetids
[1] *Blastochaetetes* sp.
[2] *Bouenia* sp.
[3] *Parachaetetes*
[4] *Ptychochaetetes globosus*
[5] *Solenopora*
[6] *Spongiomorpha ramosa*

Stromatoporoids
[1] *Actinostromina grossa*
[2] *Cladocoropsis lindstroemi*
[3] *Cladocoropsis mirabilis*
[4] *Cylicopsis verticalis*
[5] *Ellipsactinia*
[6] *Parallelopora*

Corals
[1] *Latistraea foulassensis*
[2] *Stylophyllum polycanthum*

Bivalves
[1] Ostreids
[2] *Trichites* sp.

Serpulids
[1] *Serpula socialis*
[2] *Terebella lapilloides*